Journal for ImmunoTherapy of Cancer

Mimicry-based strategy between human and commensal antigens for the development of a new family of immune therapies for cancer

Alice Talpin [1], Ana Maia [2], Jean-Marie Carpier [1], Guillaume Kulakowski [1], Lucie Aubergeon [1], Jerome Kervevan [1], Camille Gaal [1], Francesco Strozzi [1], Coline Billerey [1], Ludivine Amable [1], Tifanny Mersceman [1], Alexandrine Garnier [1], Càtia Oliveira [1], Carolina Calderon [1], Diana Bachrouche [1], Chloé Ventujol [1], Léa Bernard [1], Amandine Manteau [1], Jennifer Martinez [1], Michaël Bonnet [1], Julie Noguerol [3], Karl Laviolette [3], Laura Boullerot [4], Marine Malfroy [4], Gregoire Chevalier [1], Olivier Adotevi [4], Olivier Joffre [3], Ahmed Idbaih,[5] Maria Vieito,[6] Francois Ghiringhelli [7], Agostina Stradella,[8] Ghazaleh Tabatabai,[9] Michael C Burger,[10] Iris Mildenberger,[11] Ulrich Herrlinger,[12] David A. Reardon,[13] Wolfgang Wick,[14] Cecile Gouttefangeas [2], Christophe Bonny,[1] Laurent Chene [1], Joao Gamelas Magalhaes [1]

To cite: Talpin A, Maia A, Carpier J-M, *et al*. Mimicry-based strategy between human and commensal antigens for the development of a new family of immune therapies for cancer. *Journal for ImmunoTherapy of Cancer* 2025;**13**:e010192. doi:10.1136/jitc-2024-010192

► Additional supplemental material is published online only. To view, please visit the journal online (https://doi.org/10.1136/jitc-2024-010192).

AT, AMai, J-MC and GK contributed equally.

AT, AMai, J-MC and GK are joint first authors.

CB, LC and JGM are joint senior authors.

Accepted 28 January 2025

Check for updates

For numbered affiliations see end of article.

Correspondence to
Dr Joao Gamelas Magalhaes; jmagalhaes@enterome.com

ABSTRACT

Background Molecular mimicry between commensal bacterial antigens and tumor-associated antigens (TAAs) has shown potential in enhancing antitumor immune responses. This study leveraged this concept using commensal bacterial antigens, termed OncoMimics, to induce TAA-derived peptide (TAAp)-specific cross-reactive cytotoxic T cells and improve the efficacy of peptide-based immunotherapies.

Methods The discovery of OncoMimics primarily relied on a bioinformatics approach to identify commensal bacteria-derived peptide sequences mimicking TAAps. Several OncoMimics peptide (OMP) candidates were selected in silico based on multiple key parameters to assess their potential to elicit and ameliorate immune responses against TAAs. Selected OMPs were synthesized and tested for their affinity and stability on the major histocompatibility complex (MHC) in vitro and for their capacity to elicit cross-reactive OMP-specific/TAAp-specific CD8+T cell responses in human leukocyte antigen (HLA)-A2-humanized mice, human peripheral blood mononuclear cells (PBMC) and patients with cancer.

Results Selected OMPs demonstrated superior HLA-A2 binding affinities and stabilities compared with homologous TAAps. Vaccination of HLA-A2-humanized mice with OMPs led to the expansion of OMP-specific CD8+T cells that recognize both OMPs and homologous TAAps, exhibiting cytotoxic capacities towards tumor antigens and resulting in tumor protection in a prophylactic setting. Using PBMCs from HLA-A2+healthy donors, we confirmed the ability of OMPs to elicit potent cross-reactive OMP-specific/TAAp-specific $CD8^+$ T-cell responses. Interestingly, we observed a high prevalence of OMP-specific T cells across donors. Cytotoxicity assays revealed that OMP-stimulated human T cells specifically targeted and killed tumor cells loaded with OMPs or TAAps. Preliminary data from an ongoing clinical trial (NCT04116658) support these findings, indicating that OMPs elicit robust OMP-specific/TAAp-specific CD8+T cell responses in patients. Initial immunomonitoring data revealed sustained T-cell responses over time, with T cells maintaining a polyfunctional, cytotoxic and memory phenotype, which is critical for effective antitumor activity and long-term immune surveillance.

Conclusions These findings suggest that leveraging naturally occurring commensal-derived antigens through OMPs could significantly remodel the tumor immune landscape, offering guidance for a promising strategy for cancer peptide-based immunotherapies.

WHAT IS ALREADY KNOWN ON THIS TOPIC

⇒ Peptide-based immunotherapies have shown the potential to elicit antitumor responses; however, they often fail to induce sustained immune responses and achieve favorable clinical outcomes. Molecular mimicry, in which antigens from commensal bacteria resemble tumor-associated antigens (TAAs), has emerged as a promising approach for overcoming these challenges. Studies have suggested that mimicry between tumor and pathogen antigens could enhance the efficacy of cancer treatments. However, the application of this strategy to improve peptide-based immunotherapies remains underexplored and insufficiently validated in clinical practice.

WHAT THIS STUDY ADDS

⇒ This study outlines an innovative approach for the selection of commensal mimic peptides. We demonstrated that these peptides can effectively induce cross-reactive CD8+T cells, which specifically target and kill TAA-derived peptide (TAAp)-presenting tumor cells. Additionally, we validated the high prevalence of these OncoMimics peptides (OMPs) in inducing cross-reactive TAAp-specific T cells in the general population. Early clinical data indicated that OMPs generate robust and long-lasting cytotoxic memory T cells with a high proliferative capacity in patients with glioblastoma.

HOW THIS STUDY MIGHT AFFECT RESEARCH, PRACTICE, OR POLICY

⇒ Our findings demonstrated that molecular mimicry between OMPs and TAAps efficiently trigger cross-reactive T cells toward tumor antigens. We provide a systematic framework for the selection process and elucidate how these properties can be leveraged in cancer treatment. Our study highlights the importance of integrating molecular mimicry and T cell cross-reactivity properties to develop advanced immunotherapies targeting TAAs and by extension, tumor-specific antigens. It also provides guidance for further clinical trials to refine and validate this strategy for various types of cancers.

INTRODUCTION

Immune checkpoint inhibitors (ICIs) offer potentially curative cancer treatment by boosting anticancer T-cell immune responses in treated patients. However, their inability to stimulate specific T cells in "cold" tumors significantly limits their efficacy. Therapeutic vaccines could ideally complement ICI treatment in cancers with low mutational burdens and limited spontaneous T-cell responses.[1]

Despite the potential of therapeutic vaccines, most vaccine trials have failed, largely because of their inability to sustainably stimulate antitumor T-cell responses.[2 3] Effective induction of antitumor cytotoxic T cells (CTL) responses initially depends on the selection of appropriate tumor antigens. Typically, tumors present tumor-associated antigens (TAAs) that are shared among patients, offering broad applicability but limited immunogenicity. Tumor-specific antigens or neoantigens, not subject to thymic deletion, are theoretically highly immunogenic; however, their clinical applicability is limited due to patient specificity and rarity in low-mutational burden tumors.[4 5] We leveraged two well-described mechanisms to enhance CD8+T cell responses against tumors: peptide molecular mimicry and T cell cross-reactivity. Molecular mimicry involves using peptides from microorganisms that share sequence or structural similarities with tumor antigens, enabling the immune system to target tumor cells like microbial invaders. T cell cross-reactivity allows a single T-cell receptor (TCR) to recognize and respond to multiple peptide-major histocompatibility complexes (MHC), enabling CD8+T cells primed against microbial antigens to also target similar tumor antigens.[6 7] We developed a systematic bioinformatic approach to identify sequence similarities between bacterial and TAA peptides. The gut microbiome composition shapes the immune system and impacts vaccination and ICI therapy outcomes.[8] Furthermore, the microbiome encodes billions of "foreign" antigens that potentially maintain and trigger a memory T-cell pool at the gut level. Thus, exposure to commensal epitopes might generate rapid induction of a pre-existing pool of cross-reactive T cells, which could be leveraged to maximize the efficacy of peptide-based immunotherapies.[9 10] Taking advantage of the widespread presence of these commensal bacteria in the human population, we expected to stimulate a diverse range of memory T cells capable of cross-reacting with TAAs. By employing commensal-derived peptides (CDPs) with high affinity for human leukocyte antigen (HLA) molecules, we addressed the limited immunogenicity of TAA-derived peptides (TAAps) and aimed to activate a robust memory T-cell repertoire maintained to protect against commensal bacteria.

We describe here this approach, termed "oncomimicry", which enables the discovery of commensal-derived short peptides mimicking TAAps and eliciting potent CTL responses. The selection process for these OncoMimics peptides (OMPs) relies on various criteria, including sequence homologies between OMP and their TAAp counterparts, binding affinities to HLA class I allelic products, predicted cleavage scores and the frequencies of commensal bacterial sources expressing the selected OMPs in the human population. OMP candidates that met these criteria were tested and validated for their immunogenicity and ability to elicit cross-reacting TAAp-specific CTL responses in HLA-A2-humanized mice, resulting in tumor regression. Ex-vivo experiments showed that the identified OMPs stimulated human T-cell proliferation and triggered cytotoxic activity against target cells with homologous TAAs. Finally, initial data from an ongoing clinical trial (NCT04116658) demonstrated that OMPs generate fast, potent and long-lasting immune responses in patients, providing a strong rationale for using CDPs to enhance peptide-based immunotherapy.

MATERIAL AND METHODS

In silico OncoMimics selection

The identification process for OMP is illustrated in figure 1A and refer to the online supplemental methods section for a detailed description.

Measurement of peptide relative binding affinity for HLA-A*02:01

Peptide relative binding affinities for HLA-A*02:01 were measured as previously described with some minor modifications.[11] Briefly, T2 cells were incubated with a titration of each tested peptide and 100 ng/mL human β2-microglobulin (Sigma) in serum-free medium (TeXmacs) at 37°C for 20 hours. After incubation, the cells were washed and surface-stained with the HLA-A2 mAb (REA517). $HIVpol_{1,027–1,035}$ and $FlhA_{645–653}$ peptides were used as the positive and negative reference controls, respectively.

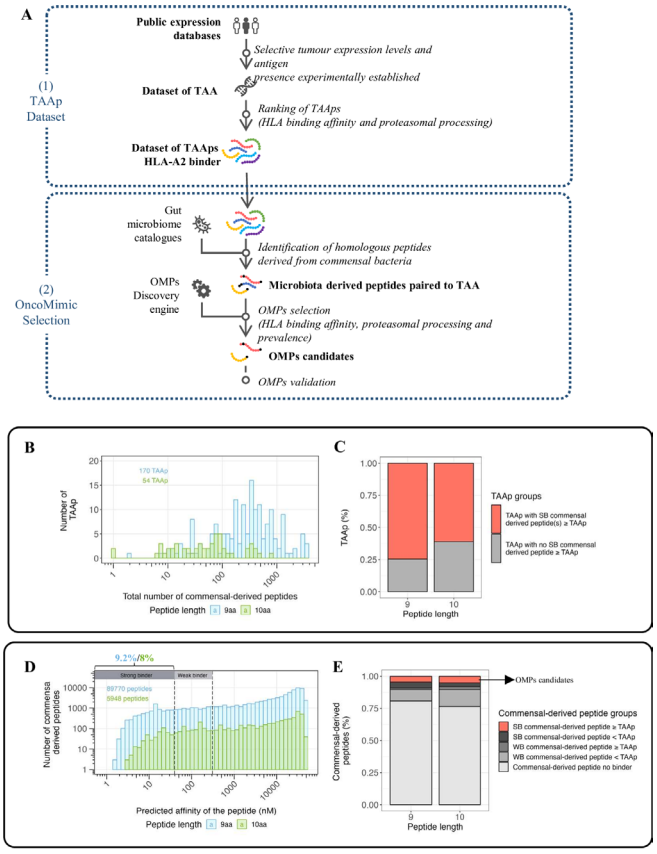

F

Tumors associated antigen derived peptides (TAAp)					Selected Commensal-derived peptides (OMPs)					
GeneID	Sequence Name	Sequence	Rank	Affinity (nM)	Sequence Name	Mismatch	Sequence	Rank	Affinity (nM)	increase affinity
IL-13R2A	IL-13R2A (345-353)	WL**PFGFI**LI	0.8	66.19	OMP16	3	F**LPFGFILPV**	0.03	4.49	14.7
BIRC5	BIRC5 (96-104)	LT**LGEFL**KL	6	2282.5	OMP17	2	F**MLGEFL**KL	0.05	5.66	403.3
FOXM1	FOXM1 (694-702)	LM**DLSTT**PL	0.5	36.19	OMP18	2	LM**DLSTT**EV	0.3	20.61	1.8
CD22	CD22 (24-32)	VV**FEHPE**TL	1	86.76	OMP64	3	Y**IFEHPE**TA	0.25	18.63	4.7
CD37	CD37 (48-56)	GL**AFVPL**QI	0.9	85.86	OMP65	2	FL**AFVPL**QL	0.05	6.02	14.3
BAFF-R	BAFF-R (77-85)	LL**FGAPA**LL	0.2	15.52	OMP66	2	LM**FGAPA**L	0.1	8.77	1.8
CD20	CD20 (118-126)	IM**NSLSL**FA	0.5	35.46	OMP72	3	A**MNSLSL**YI	0.18	12.65	2.8
UBE2C	UBE2C (124-132)	AL**YDVRT**IL	1	87.82	OMP10	2	FL**YDVRT**YL	0.01	2.75	31.9
CDC20	CDC20 (170-178)	SL**PDRIL**DA	2.5	361.75	OMP11	2	SL**PDRIL**TV	0.15	11.27	32.1
KIF2C	KIF2C (63-71)	AI**NPELL**QL	3.5	880.77	OMP12	2	AL**NPELL**AL	0.5	38.95	22.6

Figure 1 Discovery and selection process of OMPs for cancer immunotherapy. (A) OMPs discovery: A two-step process. (1) A data set of HLA-A2 peptides derived from tumor-associated antigens (TAAs) was generated from public human databases according to several parameters. (2) OMP candidates were identified by scanning each TAA-derived peptide against all peptide sequences of the same length from gut microbiome catalogs using different homology criteria (detailed in online supplemental M&M). (B) TAA-derived peptides distribution based on the number of their commensal-derived peptides: the graph shows the distribution of 224 TAA-derived peptides (TAAps) based on the number of their associated CDPs. (C) Repartition of TAA-derived peptides based on the HLA-A2 affinities of their commensal-derived peptides: the graph represents the repartition of TAA-derived peptides based on two categories: TAAp with strong binder (SB) CDPs≥TAAp or TAAp with no SB strong binder CDPs≥TAAp. In other words, the presence (in red) or absence (in gray) of at least one strong binder CDP, is stronger than its TAAp counterparts. In the legends of figure 1C and E, the symbol "≥" indicates "a stronger predicted affinity than", while "<" signifies "a weaker predicted affinity than". (D) Commensal-derived peptide distribution based on HLA-A2 predicted binding affinities: the graph shows the distribution of commensal-derived peptides based on their HLA-A2 predicted binding affinity. Commensal-derived peptides with the highest affinities (lower nanomolar values) are shown on the left side of the graph. We classified the CDPs into three categories based on their %rank (according to NetMHCpan3.0 recommendations): strong binders (SB) were defined as having %rank<0.5, weak binders (WB) with %rank<2 and no binder peptides with %rank>2. (E) Commensal-derived peptide repartition based on their HLA-A2 predicted binding affinity compared with their TAAp counterparts: The graph shows how commensal-derived peptides are categorized into five groups: SB commensal-derived peptide with an HLA-A2 affinity equal to or stronger than the associated TAAp; SB commensal-derived peptide with an HLA-A2 affinity equal to or weaker than the associated TAAp; WB commensal-derived peptide with an HLA-A2 affinity equal to or stronger than the associated TAAp; WB commensal-derived peptide with an HLA-A2 affinity equal to or weaker than the associated TAAp; Commensal-derived peptides that are no binders to HLA-A2. (F) Characteristics of the 10 selected HLA-A2 OMPs in this study and their homologous TAAps: gene ID of the targeted TAA, sequence name of TAAp and corresponding OMP. Amino acid (aa) sequences predicted affinity rank and binding affinity (nM) to HLA-A*02:01 molecule of each pair and the numbers of mismatches are shown. Amino acid substitutions are indicated in red and those in dark bold are the five amino acids in the peptide core. Fold increases in affinity between OMP and corresponding TAAp. CDPs, commensal-derived peptide; HLA, human leukocyte antigen; OMP, OncoMimics peptide.

The geometric mean fluorescence intensities of HLA-A2 staining were measured by flow cytometry (MACSQuant analyzers, Miltenyi Biotec) to determine the percentage of HLA-A*02:01 molecules stabilized at the cell surface, as follows:

$$\%\ HLA\_A2\ binding = \frac{GeoMFI\ obtained\ with\ tested\ peptide - GeoMFI\ obtained\ with\ FlhA645\_653\ x100}{GeoMFI\ obtained\ with\ HIVpol1027\_1035 - GeoMFI\ FlhA645\_653}$$

The relative affinity (RA) of each peptide for HLA-A*02:01 was determined as the ratio of the peptide concentration to the reference peptide concentration (HIV) that stabilized 20% of the HLA-A2 signal at the cell surface. The lower the RA, the stronger the peptide binding to HLA-A*02:01.

$$RA = \frac{Concentration\ of\ candidate\ peptide\ that\ stabilizes\ 20\%\ of\ the\ HLA{*}02{:}\ 01\ expression}{Concentration\ of\ HIV\ peptide\ that\ stabilizes\ 20\%\ of\ the\ HLA-A{*}02{:}\ 01\ expression}$$

Assessment of peptide/HLA-A*02:01 complex stability

The stability of peptide binding to HLA-A*02:01 was measured using T2 cells pulsed overnight with individual peptides and human β2-microglobulin, followed by the indicated chase kinetics performed in the presence of Brefeldin A (Sigma) to inhibit the neosynthesis of HLA-A*02:01, as previously described.[11] The dissociation complex at 50% (DC50) was defined as the half-life of the peptide-MHC complex and was calculated as the time required to observe 50% decay of the initially stabilized peptide-MHC complex.

Animal models

All experimental protocols were approved by the local Ethics Committee on Animal Experimentation and followed the guidelines of the EU. For Enterome, approvals were from CEEA N°51, CERFE (D91228107), and APAFIS (#35 017–2021101316078260 v7). At the Université de Franche-Comté, approvals were from the local Animal Ethics Committee (#58) and APAFIS (#2021–004-OA-12PR). Both received validation from the French Ministry of Higher Education, Research and Innovation, and the French Ministry of Agriculture. The previously described HLA-DRB1*01:01/HLA-A*02:01-transgenic mice (A2/DR1 mice), H-2 class I and II knockout animals were obtained from Francois Lemonnier (Institut Pasteur, Paris, France).[12] $CD8^+$ and $CD4^+$ T cells were restricted to HLA-A*02:01 and HLA-DR1*01:01, respectively. All the mice used in the described studies were bred and maintained under specific pathogen-free conditions at Charles River Laboratories.

A2/DR1 prime-boost immunizations

Mice were immunized on days 0 (prime) and 14 (boost) with the indicated MHC class I peptides (5, 30, or 95 nmol per mouse) and MHC class II helper peptide (universal cancer peptide 2 (UCP2), 30–100 µg per mouse) emulsified in Montanide ISA 51 VG (ratio 50:50, Seppic). Immunization was performed subcutaneously using 100 µL of the emulsified preparation.

Restimulation of peptide-specific $CD8^+$ mouse T cells ex vivo postimmunization

To determine the immunogenicity of the analyzed peptides and the cross-reactivity of specific T cells against human TAA homologs, mice were euthanized 21 days post-prime immunization and the number of IFN-γ peptide-specific $CD8^+$ T cells in the spleen of the animals was determined by Enzyme-Linked ImmunoSpot (ELISpot) (Mabtech, 3321-4APT-2 kit) following the manufacturer's recommendations. Briefly, spleens were harvested and mechanically disrupted and red blood cells (RBCs) were lysed with RBC lysis buffer (Miltenyi Biotec). 2×10^5 splenocytes were restimulated per ELISpot well using the indicated peptides at a concentration of 10 µM. PMA (Phorbol-myristate acetate, 0.1 µM, Sigma) and ionomycin (1 µM, Sigma) were used as positive controls and EZH2-B2, an HLA-A2:01-restricted peptide, was used as a negative control. Cells were cultured for approximately 20 hours in media (Roswell Park Memorial Institute (RPMI)-1640 (Sigma), 10% fetal bovine serum (VWR), 1% GlutaMAX (Gibco), 1% non-essential amino acid (aa) (Sigma), 10 mM HEPES (Sigma), 1 mM sodium pyruvate (Sigma)+1% penicillin/streptomycin (PenStrep) (Sigma), 50 µM β-mercaptoethanol (β-ME) (Sigma)) and respective peptides at 37°C and 5% CO_2. IFN-γ spots were detected according to the manufacturer's instructions and counted using an iSpot ELISpot Fluorospot reader system (AID). The number of spots obtained for each mouse and each condition was subtracted from the background values (cells cultured in media only) and normalized to the frequency of total T cells from each mouse, resulting in the number of specific IFN-γ-producing T cells/10^6 T cells.

Tumor protection model

After prime-boost immunization, A2/DR1 mice were subcutaneously injected 21 days post-prime immunization in the right flank with 0.5×10^6 SARC-A2-hCD20-GFP or SARC-A2-GFP sarcoma cells resuspended in phosphate-buffered saline (PBS). Tumor growth was evaluated twice a week using a caliper and the mice were euthanized when their tumors reached a volume≥300 mm^2.

In vivo cytotoxicity in humanized HLA-A2 mice

To test the cytotoxic function of $CD8^+$ T cells that were activated following vaccination, immunized A2/DR1 mice were challenged 6 days post-boost immunization with syngeneic splenocytes pulsed with either a mix of peptides or individual peptides. Unimmunized A2/DR1 donor mice were euthanized and a suspension of syngeneic splenocytes was prepared. To assess the cytotoxic response against peptide pools, splenocytes were split into two fractions and labeled with a cell tracking dye (Carboxyfluorescein Succinimidyl Ester (CFSE) or Cell Trace Violet, Thermo Fisher Scientific) using a low (0.3 µM) or a high concentration (3 µM). To determine the individual contribution of each peptide, refer to online supplemental materials. The bright populations used as target cells were pulsed for 2 hour at 37°C with a peptide

pool or a specific peptide at a final concentration of 100 µM before being mixed at an equal ratio with the other populations. Cells were injected intravenously into immunized and naïve mice and the in vivo cytotoxic response was assessed 20 hours post-injection. Antigen-specific lysis was calculated as follows:

$$\%\ \text{Specific lysis} = \frac{\%\ \text{of targeT cells in naive mice} - \%\ \text{of target in immunized mice}\ \times 100}{\%\ \text{of targeT cells in naive mice}}$$

Generation of antigen-specific CD8+ CTL in HLA-A*0201 HD PBMCs

Peripheral blood mononuclear cells (PBMCs) were stimulated for 24 hours with OMPs at 10 µM in ImmunoCult medium (STEMCELL). Antigen-specific T cells were enriched by magnetic isolation using a CD137-VioBright-Fluorescein Isothiocyanate (FITC) mAb (REA765, Miltenyi Biotec), anti-FITC microbeads and LS MACS columns (Miltenyi Biotec) as previously described.[13] After CD137 enrichment, polyclonal T cell expansion was performed for 8 days with ImmunoCult Human CD3/CD28 T Cell Activator (STEMCELL) in expansion media (ImmunoCult culture medium supplemented with IL-2 (50 U/mL), IL-7 (12.5 ng/mL), IL-15 (12.5 ng/mL) and IL-21 (62.5 ng/mL) (all from Miltenyi Biotec)). Cells were then restimulated every 10 days using peptide-loaded T2 cells (APCs) at a ratio of 10:1 in the expansion medium, as previously described.[14] Before co-culture, T2 cells were treated for 1 hour with Mitomycin C (Sigma) at 20 µg/mL, washed and loaded with 100 ng/mL β2-microglobulin (Sigma) and 10 µM peptides overnight. The frequency of antigen-specific CD8+ T cells was assessed by surface staining with CD8 VioGreen mAb (REA734) and fluorescently labeled tetramers. The percentage of cross-reactivity of each healthy donor (HD) (%) was calculated as follows:

$$\%\,cross-reactivity = 100 - \left[\frac{(\%\ TAA-specific\ CD8{+}T\ cells)\ x100}{\%\ OMP-specific\ CD8{+}T\ cells}\right]$$

Flow cytometry-based cytotoxicity assay in HLA-A*0201 HD PBMCs

T2 target cells were labeled with the CellTrace Far Red Proliferation Kit (Thermo Fisher Scientific) and loaded overnight with 10 µM of the individual peptide and 100 ng/mL β2-microglobulin. Peptide-loaded target cells were co-cultured with peptide-specific CD8+ T cells at 37°C for 24 hours.[15] Media and EZH2-B2 irrelevant peptides were used as the negative controls. Antigen-specific CD8+ T cells were stained with VioGreen or PerCPVio700 CD8 mAbs (REA734) and dead cells were identified using the LIVE/DEAD Fixable Violet Dead Cell Stain Kit. Conditions were performed in duplicate and SD were calculated. The percentage of specific cell killing was calculated as follows:

$$\%\,cytotoxicty = 100 - \left[\frac{(live\ T2\ cells\ cocultured\ with\ CD8\ T\ cells)\ x100}{Live\ T2\ cells\ only}\right]$$

Statistical analyses were performed using the GraphPad Prism (V.8).

Immunomonitoring protocols

Tetramer staining assay and memory phenotype analyses in patients

Tetramer staining was performed ex vivo on thawed PBMCs and/or cells that had been subjected to in vitro stimulation (IVS). Cells were washed with Fluorescence-Activated Cell Sorting (FACS) Buffer (PBS supplemented with 2% Fetal Calf Serum (FCS), 0.02% Sodium Azide (NaN_3) and 2 mM EDTA) and incubated with two separate tetramer mixes (one containing OMPs and the other containing TAAp-tetramers) each at 2.5 µg/mL for 30 min at room temperature (RT). In some experiments, PBMCs were also incubated with three separate mixes, each containing matched OMP and TAAp tetramers, to assess T cell cross-reactivity. The tetramers were diluted in PBS supplemented with 0.02% NaN_3, 2 mM EDTA and 50% FCS for staining. The cells were then washed once with FACS buffer and incubated with mAbs against CD4 (APC-Cy7, BD Biosciences), CD8 (PE-Cy7, Beckman Coulter), CD14 and CD19 (both PerCP, BioLegend) for 20 min at 4°C. A dead live-cell marker (Zombie Aqua, BioLegend) was also included. In the ex vivo setting, mAbs against CD45RA (FITC, BD Biosciences) and CCR7 (BV650, BioLegend) were included in the staining mix to evaluate the naïve/memory/effector phenotypes of the antigen-specific CD8+ T cells. After three washes, the samples were analyzed using an LSRFortessa Cell Analyzer (Becton Dickinson). At least 750,000 and 600,000 cells were acquired in the ex vivo and IVS settings, respectively. The data were analyzed using FlowJo V.10. Tetramer+ T cells were presented as the percentage of cells within living CD8+ lymphocytes. For the analysis of the naïve/memory/effector phenotype, the results are shown as the percentage of cells within tetramer+ CD8+ cells.

IVS of patient PBMCs

PBMCs from patients were expanded for 12 days IVS with the bacterial peptide pool (EO2316, EO2317 and EO2318) before analysis by tetramer staining, IFN-γ ELISpot assay and intracellular staining assay.[16] For the expansion procedure, PBMCs were thawed in a thawing Iscove's Modified Dulbecco's Medium (IMDM (Gibco) supplemented with 2.5% heat-inactivated human serum (HS, Capricorn), 1% PenStrep solution (Sigma), 50 µM β-ME and 3 µg/mL DNase I (Sigma)), washed (1300 rpm, 8 min, RT), counted and resuspended in dedicated medium (IMDM supplemented with 10% HS, 1% PenStrep and 50 µM β-ME, hereafter referred to as TCM). Cells were seeded either in 24 or 48 well plates at approximately $2.5–3.5\times10^6$ cells per well and cultured for 24 hours (37°C, 5% CO_2). On day 1, peptides were added to the culture medium (final concentration of 1 µg/mL for each OMP). On day 3, IL-2 was added to the culture medium (final concentration of 2 ng/mL; rhIL-2 reference: R&D 202-IL-010). On day 5, the cells were split

by 1/3 and 2 ng/mL IL-2 was added again. On days 7 and 9, the medium was removed from each well and replaced with fresh TCM medium containing IL-2 (2 ng/mL). If necessary, the cells were split in a 1:2 ratio on day 9. On day 12, the cells were collected and their viability and number were assessed with an automated cell counter (Nucleo Counter NC-250) using an Acridine Orange-4′,6-Diamidino-2-Phenylindole (AO-DAPI) staining reagent (solution 18 from ChemoMetec).[17]

IFN-γ ELISpot assay for patient T cells

For the ELISpot assay, after 12 days of IVS with OMP pools, cells were collected and plated in ELISpot plates (Merck Millipore) pre-coated with a monoclonal anti-IFN-γ mAb (clone 1-D1K purified Mabtech) at a density of 200,000 cells/well. Cells were incubated with the human peptide pool (IL-13RA2, BIRC5 and FOXM1 at 5 µg/mL each) or individual bacterial peptides (EO2316, EO2317, or EO2318, each at 1 µg/mL) for 26 hours. A peptide solvent (10% Dimethyl Sulfoxide (DMSO) in water) was used as the negative control. Phytohemagglutinin (PHA) at 10 µg/mL was used as the positive control. After incubation for 26 hours, the cells were discarded and IFN-γ was detected by adding anti-human IFN-γ biotinylated mAb (clone 7-B6-1, Mabtech) for 2 hours, followed by incubation with ExtrAvidin Alkaline Phosphatase (Sigma) for 1 hour and finally, 5-Bromo-4-Chloro-3-Indolyl Phosphate/Nitro Blue Tetrazolium (BCIP/NBT) substrate (Sigma) was added to the wells. Plates were left to dry for at least 12 hours at RT in the dark prior to plate imaging and spot counting using an Immunospot S6 Universal Analyzer (CTL). The number of spots in peptide-stimulated wells (n=3 for each condition) was compared with those obtained in the negative control (solvent control wells) using a permutation test (distribution-free resampling DFR2x).[18] If less than three replicates per condition were available, analyses were performed manually based on positivity criteria from the laboratory (at least twice the spot count in peptide-stimulated wells compared with the solvent control plus a minimum of 6 spots per 100,000 cells seeded).

Cytotoxicity assay on glioblastoma cell lines

PBMCs from the three vaccinated patients were stimulated in vitro with OMP peptides (EO2316, EO2317 and EO2318) for 12 days as described above. Cells were then stained with TAAp-tetramers and the $CD8^+$ T cells specific for IL13RA2, BIRC5 and FOXM1 were isolated with a BD Influx Cell Sorter. Sorted cells were polyclonally amplified using ImmunoCult Human CD3/CD28 T Cell Activator (STEMCELL) in expansion media (ImmunoCult culture medium supplemented with IL-2 (50 U/mL), IL-7 (12,5 ng/mL), IL-15 (12,5 ng/mL) and IL-21 (62,5 ng/mL) (all from Miltenyi Biotec)). To perform the cytotoxic assay, U87 (HLA-A2+) and U118 (HLA-A2-) cell lines were labeled with CellTrace Violet (Thermo Fisher Scientific) and co-cultured with the amplified TAAp-specific $CD8^+$ T cells at 37°C for 24 hours in 50% RPMI/50% X-vivo 15 media at different effector-to-target cell (E:T) ratios. T2 target cells were labeled with CellTrace Violet and co-cultured with the amplified TAAp-specific CD8+T cells, peptides (OMPs or irrelevant EZH2 control peptide) and β2-microglobulin at 37°C for 24 hours in 50% RPMI (Gibco)/50% X-vivo 15 (Lonza) media. Media and EZH2-B2 irrelevant peptides were used as negative controls. Specific CD8+T cells were stained using AF700 CD8 (clone SK1, BioLegend) mAb, and dead cells were identified using the LIVE/DEAD Fixable Near-IR Dead Cell Stain Kit. Conditions were performed in duplicate. The percentage of specific cell lysis was calculated as follows:

$$\%\,cytotoxicty = 100 - \left[\frac{(Live\ target\ cells\ cocultured\ with\ CD8\ T\ cells)\ x100}{Live\ target\ cells\ only}\right]$$

Statistical analysis

Results are expressed as mean±SEM or SD. The Mann-Whitney U test was used to compare the two groups. Comparisons between tumor growth curves were performed using a two-way analysis of variance test and multiple comparisons were corrected using the Bonferroni coefficient. Statistical significance was determined using Prism software (GraphPad software). Statistical significance was set at $p<0.05$.

RESULTS

Comprehensive multistep process for discovering and selecting OMPs for cancer immunotherapy

We developed a comprehensive bioinformatic pipeline to identify CDPs that exhibit molecular mimicry (sequence similarities) with TAAps. This approach targets peptides with enhanced affinity for HLA class I molecules, particularly HLA-A2, owing to its prevalence in approximately 49% of the Caucasian population, with a significant majority expressing the HLA-A*02:01 allelic variant.[19] Our strategy was to identify immunogenic CDPs capable of initiating cross-reactive CD8+T cell responses against cancer cells presenting these TAAps. We screened 224 HLA-A2 verified TAAps derived from 113 well-described TAAs against a large public database of gut commensal proteins (online supplemental table 1 and online supplemental M&M). This database comprises almost 10 million genes from 1267 individuals, highlighting the potential of the gut microbiome as a source of short peptides that can potentially mimic all described MHC class I tumor peptides.[20] Peptide pairs (CDP/TAAp) were selected according to criteria aimed at maximizing aa changes that improve HLA-A2 binding affinity (anchor positions) while maintaining strict identity within the central aa sequence (core positions) crucial for TCR recognition when presented by MHC class I (figure 1A).[21]

Our screening identified 95,718 CDPs as potential matches, with the number of CDPs per TAAp ranging from 1 to 3,543 (figure 1B, online supplemental table 2). 74.7% of the 9-mers and 61.1% of the 10-mers from the selected TAAps queries returned at least one strong

binder (SB) HLA-A2 CDP with enhanced binding properties, demonstrating that the majority of the well-documented HLA-A2 TAAps have at least one SB CDP equivalent (figure 1C). Among all CDPs, 9.2% of 9-mers and 8.0% of 10-mers were predicted to be SB (figure 1D), with 4.6% predicted to have higher affinities than their TAAp counterparts. We designated this high-affinity CDPs subset as OMP candidates, meeting our criteria for sequence homology with TAAps and exhibiting increased HLA-A2 affinities (figure 1E).

10 OMPs were selected to assess their biological potential. Six OMP-matched TAAps derived from overexpressed tumor antigens (IL-13RA2, BIRC5, FOXM1, UBE2C, CDC20 and KIF2C) prevalent in solid tumors such as glioblastoma, lung, breast and colorectal cancers have been identified as key tumor drivers.[22–27] While these six TAAs are associated with a range of solid tumors, IL13RA2, BIRC5, and FOXM1 are ideal targets for immunotherapy in patients with glioblastoma. IL13RA2, BIRC5, and FOXM1 are overexpressed in glioblastoma tissue and play critical roles in tumor progression. All three proteins are found overexpressed in a large fraction of glioblastomas (60–85%) and contribute to the survival of tumor cells, being associated with poor prognosis. The remaining four OMPs matched TAAps derived from CD22, CD37, BAFF-R and CD20, which are B cell surface markers, used as targets in B cell lymphoma therapies.[28] These 10 OMPs were selected from a comprehensive pool of candidates, distinguished as the most promising based on several parameters. This included sequence similarity to TAAps to retain molecular mimicry, high HLA-A2 binding affinity, prediction of potent immunogenicity, likelihood of proteasomal processing and prevalence within the gut microbiome to augment the probability of a responsive T cell repertoire (online supplemental table 2and online supplemental M&M for details). The selected OMPs presented two or three aa mismatches and exhibited significantly enhanced predictive affinities, ranging from 1.8-fold to 400-fold higher than those of their TAAp counterparts (figure 1F). This selection process aims to predict whether these OMPs can trigger strong immune responses in a wide population segment.

OMPs induce cross-reactive T-cell responses in vivo

To validate the in silico HLA-A2 affinity predictions, we used a TAP-deficient HLA-A*02:01-positive T2 cell line. These cells provided an established model to assess peptide-HLA-A2 binding (online supplemental figure 1A). Our in vitro binding assays revealed that each tested OMP exhibited enhanced binding affinity compared with the corresponding TAAp (figure 2A, online supplemental figure 1B,C). Peptide-HLA-A2 stability assay further highlighted that OMP/HLA-A2 complexes were significantly more stable than their TAAp/HLA-A2 counterparts, with dissociation half-life complex (DC50) values ranging from 2 hours to more than 24 hours (figure 2B, online supplemental figure 1B and D). This enhanced stability suggests prolonged antigen presentation, potentially improving T cell recognition and response. The immunogenicity capacity and ability of OMPs to induce cross-reactive T cells were subsequently investigated in vivo using humanized HLA-A2-DR1 transgenic mice. On OMP immunization, antigen-specific IFN-γ T cell responses were evaluated (figure 2C). Robust T cell responses, defined as exceeding 1,000 IFN-γ SFU (Spot-Forming Unit) per 10^6 total T cells, were observed for all OMPs tested, while no activation was detected in naïve mice. The induction of cross-reactive T-cell responses was further confirmed by the capacity of OMP-induced T cells to produce IFN-γ on ex vivo restimulation with the corresponding TAAps (figure 2D, online supplemental figure 1E). The number of T cells responding to OMPs and TAAps restimulation on OMPs immunization in individual mice strongly correlates, with a Pearson coefficient ranging from 0.42 for the least correlated peptide pair, OMP10/UBE2C, to 0.99 for the most correlated pair OMP66/BAFF-R. 7 out of 10 peptide pairs showed strong correlations (≥0.80) (online supplemental figure 1F). Cross-reactivity levels, defined as the percentage of OMP-induced T cells that recognize corresponding TAAps, ranged from 13.8% (OMP16/IL-13RA2) to 82.2% (OMP66/BAFF-R) (figure 2D). Based on OMPs capacity to induce TAAp-specific responses, representing the ratio between OMP immunogenicity and cross-reactivity capacity, we observed the OMP65/CD37, OMP66/BAFF-R and OMP17/BIRC5 induce high TAAp-specific IFN-γ responses (>5,000 SFU) and cross-reactivity levels (≥75%). OMP12/KIF2C, OMP11/CDC20, OMP72/CD20 and OMP10/UBE2C induce lower TAAp-specific IFN-γ responses (2,000–5,000 SFU) and cross-reactivity levels ranging from 30% to 80%. Lastly, OMP64/CD22, OMP18/FOXM1 and OMP16/IL-13RA2 induce lower TAAp-specific responses (<2,000 SFU) and cross-reactivity levels≤20% (except OMP64). Overall, these results reveal the capability of OMPs to induce strong IFN-γ-producing T cell responses, recognizing both peptides (OMPs and TAAps). Mice were then immunized with either OMPs or TAAps and T cells were restimulated ex vivo with either peptide (figure 2E). T cell responses against KIF2C, IL-13RA2, BIRC5, CD37 and BAFF-R peptides were weaker when mice were immunized with TAAps than with their mimic OMPs, demonstrating superior immunogenicity for OMP12, OMP16, OMP17, OMP65 and OMP66 over their homologous TAAps (figure 2F, top panel). For CDC20-specific, CD20-specific and UBE2C-specific T-cell responses, the magnitudes were similar, regardless of the initial vaccination (figure 2F, middle panel). Only CD22-specific and FOXM1-specific T-cell responses were weaker after OMP immunization than after TAAp immunization (figure 2F, bottom panel). Additionally, OMP-specific responses induced by OMP immunization were consistently stronger than those induced by TAAp immunization, except for the OMP64/CD22 pair, which showed similar levels (figure 2F).

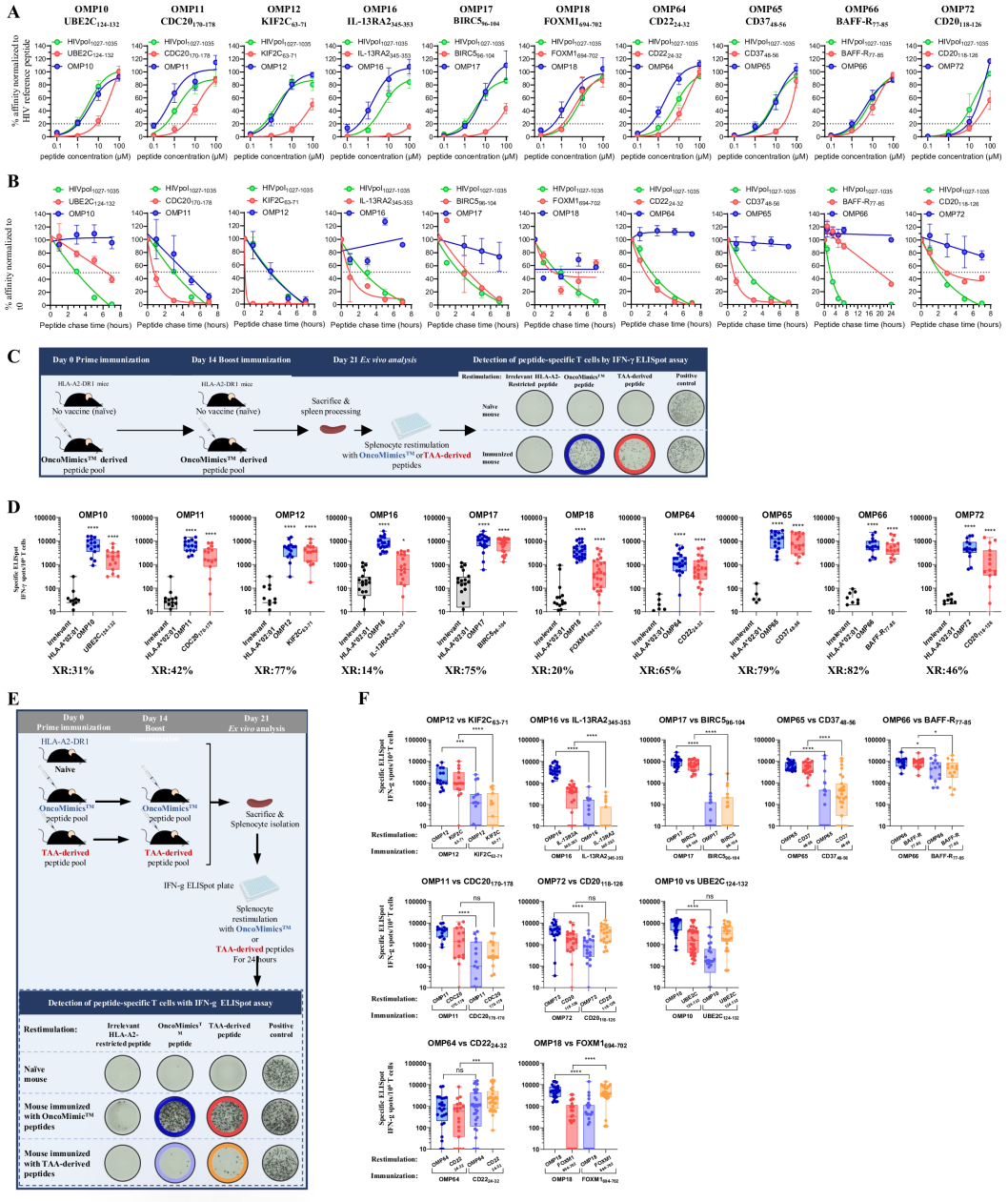

Figure 2 OMPs selected in vitro for their HLA-A2 binding and stability properties and in vivo for their immunogenicity are capable of eliciting potent cross-reactive responses in HLA-A2/DR1 mice. (A, B) Binding and stability of TAA-derived peptides and their OMP counterparts. Comparison of HLA-A2 binding (A) and stability (B) of TAA-derived peptides (red), their OMP counterparts (blue) and the HIV reference peptide (green) in the T2-binding assay. The data represent four to seven independent experiments. Symbols represent the mean and error bars indicate the SEM. (C) Schematic representation of the in vivo experimental setup used to assess OMPs immunogenicity and $CD8^+$ T cell-dependent cross-reactive responses against TAAps. (D) In vivo immunogenicity and cross-reactivity. The frequency of peptide-specific T cells that produce IFN-γ was determined by ELISpot analysis of splenocytes from mice vaccinated with the indicated peptides. The negative control, OMP and TAAp are shown in gray, blue and red, respectively. Below each graph, the percentages of cross-reactivity (XR) between OMP and its TAA counterpart are displayed. (E) Schematic representation of the in vivo experimental set-up used to compare the capacity of OMPs and TAA-derived peptides to induce a TAAp-specific response. (F) OMP-induced and TAAp-induced cross-reactive responses. Comparison of OMP efficacy in inducing a TAAp-specific response to that of their TAA counterparts in A2/DR1 humanized mice assessed on splenocytes from mice immunized with the indicated peptides by IFN-γ ELISpot assay. Dark blue, red, light blue and orange indicate OMP vaccination and restimulation conditions, OMP vaccination and TAAp restimulation, TAAp vaccination and OMP restimulation conditions and TAAp vaccination and restimulation conditions, respectively. The data shown in (D) and (F) are from one to five independent experiments; symbols indicate individual mice (n=5–25 mice) and bars represent min and max values. Statistical comparisons were performed using an unpaired non-parametric test (Mann-Whitney). *p<0.05, **p<0.001, ****p<0.0001, ns: non-significant. ELISpot, Enzyme-Linked ImmunoSpot; HLA, human leukocyte antigen; OMP, OncoMimics peptide, TAA, tumor-associated antigen.

OMPs trigger CTL responses with antitumor activity

The in vivo cytotoxicity of the OMP-triggered T cells was investigated using a fluorescence-based CTL assay. Following a prime/boost immunization of A2/DR1 mice with the OMP pools (OMP17, OMP18, OMP10, OMP11, OMP12) or (OMP64, OMP65, OMP66, OMP72), a 1:1 ratio of syngeneic splenocytes loaded with the corresponding OMPs (bright labeling) and unloaded (dim labeling) were injected into immunized or control animals (figure 3A). Flow cytometry analysis, conducted 20 hours post-injection, demonstrated that OMP-induced T cells exhibited substantial cytotoxic activity towards OMP-loaded target cells without affecting control cell viability, indicating that OMPs elicit robust OMP-specific CTL responses (figure 3B). Individual OMP-specific CTL activity was observed against T2 cells loaded with most of the OMPs tested, although the CTL activity against OMP64 was lower and the one against OMP72 was negligible (online supplemental figure 2A,B). More importantly, OMP-specific CTL responses induced by OMPs were TAAp-specific. Splenocytes loaded with matched TAAps pool (BIRC5, FOXM1, UBE2C, CDC20 and KIF2C) or (CD22, CD37, BAFF-R and CD20) were efficiently killed, demonstrating the OMP/TAAp cross-reactivity of the OMP induced T cells in vivo (figure 3C).

To further explore the OMP-induced TAAp-specific CTL activity in vivo, we established a tumor protection model using the syngeneic HLA-A2$^+$ sarcoma cell line (SARC-A2), as it is the only compatible tumor cell line available for the A2/DR1 mouse model.[29] Attempts to develop SARC-A2 constructs with ectopically expressed TAAs were unsuccessful due to rapid TAA expression loss or spontaneous tumor rejection, limiting our preclinical studies. However, SARC-A2 engineered to express the human CD20 antigen as well as GFP (SARC-A2-GFP-hCD20) demonstrated sufficient stability and did not undergo spontaneous rejection, allowing short-term implantation experiments. We established a tumor protection model using SARC-A2-GFP-hCD20 and the GFP-alone control cell line (SARC-A2-GFP) (figure 3D). This approach allowed us to assess the capacity of OMP72 to trigger CD20-targeted CTL-mediated tumor cell killing. After immunization with OMP72, half of the A2/DR1 mice engrafted with SARC-A2-GFP-hCD20 tumor cells exhibited tumor protection compared with the control groups (figure 3E,F). Interestingly, in mice in which tumor control was not achieved, we observed a loss of CD20 surface expression in 99% of the tumor cells, suggesting a potential escape mechanism from OMP72-specific T-cell surveillance (figure 3G). Supporting this hypothesis, comparable levels of OMP72-specific IFN-γ-producing cells were measured in both responsive and non-responsive mice, indicating no significant difference in the immune response induced in either group (figure 3H). Altogether, these results demonstrate the ability of OMPs to induce OMP-/TAAp-specific CTL activity in vivo.

OMP-specific T cells represent a prevalent pool of T cells in the human population

The ability of OMPs to induce efficient TAAp-specific cross-reactive CTL responses was evaluated in human PBMCs isolated from HLA-A2$^+$ HDs and stimulated in vitro in the presence of OMPs (figure 4A). Flow cytometry analysis using peptide-MHC tetramers revealed that all OMPs induced cross-reactive OMP-/TAAp-specific CD8$^+$ T cells (online supplemental figure 3A–C). Within the same OMP/TAAp pair, the extent of cross-reactivity varied among different HD PBMCs, ranging from 10% to 100%. On average, some OMP/TAAp pairs showed cross-reactivity levels below 33% (OMP10, OMP11, OMP18, OMP64), some between 33% and 66% (OMP16, OMP65, OMP66, OMP72) and some above 66% (OMP12, OMP17), compared with the total elicited OMP-specific T cell responses (online supplemental figure 3D). This pattern emphasizes variability not only within individual responses to the same OMP/TAAp pair, but also across different OMP/TAAp pairs. OMP-amplified human T cells effectively recognized and destroyed OMP-loaded T2 target cells, whereas control T2 cells (pulsed with irrelevant peptides or unloaded) were untouched, confirming the specificity of the killing activity. More importantly, OMP-expanded human T cells also killed T2 cells loaded with matched TAAps, demonstrating the TAAp-specific CTL activity of these T cell clones. Reduced and variable cytotoxic values were observed for IL-13RA2, likely because of the low affinity of the IL-13RA2 peptide and its poor stability when loaded onto T2 cells (figure 4B). In most cases, killing occurs at a low E:T ratio of 1:10, strengthening the efficacious functional cytotoxic activity of these effector cells. Moreover, OMP-specific T cells killed OMP-loaded and TAAp-loaded T2 cells with equal efficiencies (figure 4B). We further determined the prevalence of OMP-specific CD8$^+$ T cells in the human population. Notably, all OMP-specific CD8$^+$ T cells were detected in>79% of HLA-A2$^+$ PBMCs samples, except for OMP64, which showed a prevalence of 67% (figure 4C). This high detection rate emphasizes the widespread potential of OMPs to engage the immune system across a broad segment of the population, thereby highlighting their relevance in immunotherapeutic strategies against cancer.

OMPs induce fast, strong and long-lasting polyfunctional T-cell responses in patients with cancer with recurrent glioblastoma

Immune responses induced by OMPs were evaluated in patients in the EOGBM1-18/ROSALIE clinical trial (NCT04116658). EOGBM1-18 is a first-in-human phase Ib/IIa trial in patients with the first recurrence of glioblastoma after a radiotherapy/Temozolomide (TMZ) regimen. The patients received immunotherapy, designated as EO2401, comprizing three OMPs (EO2316/OMP16 mimicking the IL-13R2A$_{(345–353)}$ peptide, EO2317/OMP17 mimicking the BIRC5$_{(96–104)}$ peptide, and EO2318/OMP18 mimicking the FOXM1$_{(694–702)}$ peptide)

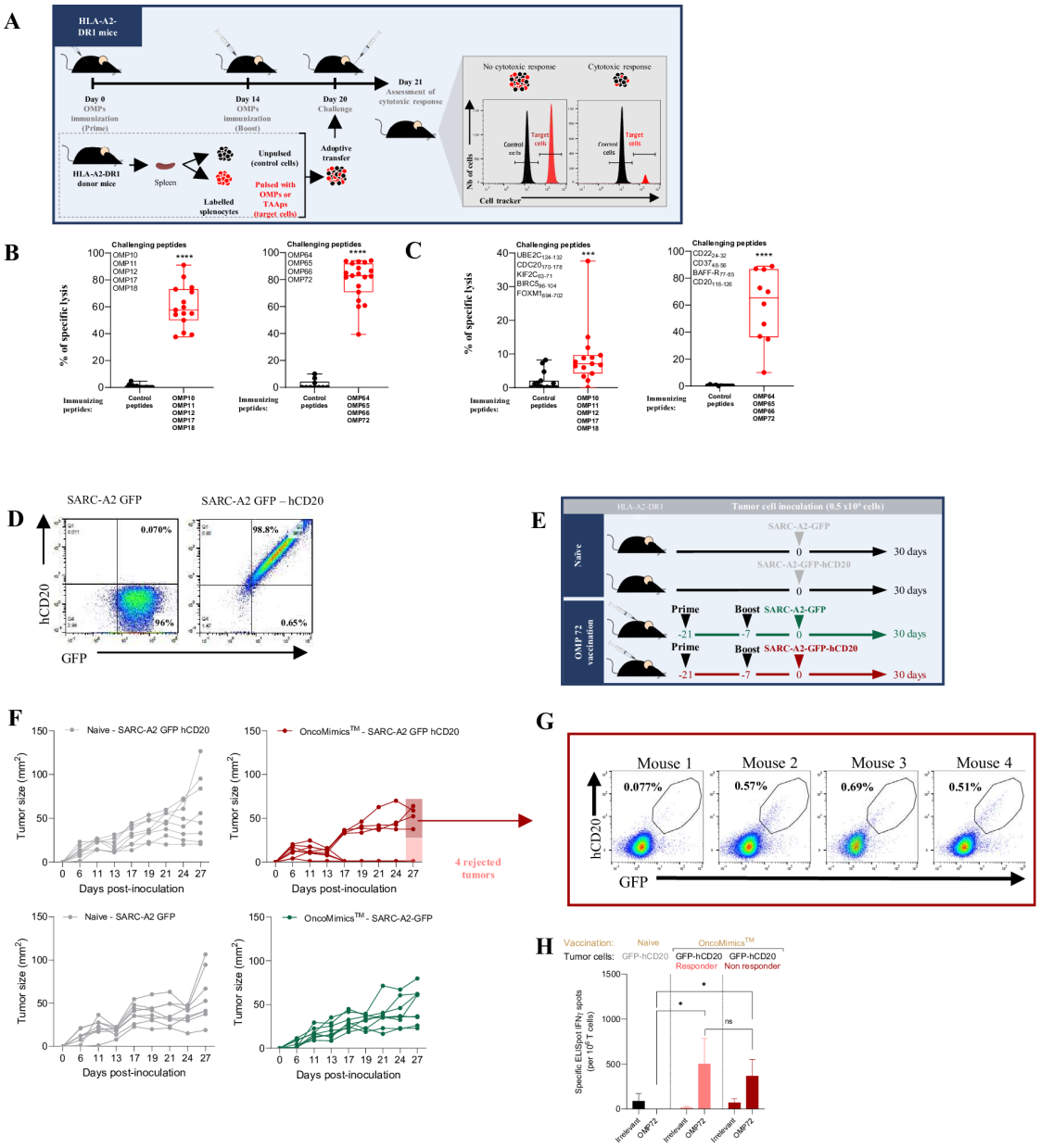

Figure 3 OMP-based vaccines elicit functional cytotoxic T cells in mice that are cross-reactive with human TAA-derived peptides in vivo. (A) Schematic representation of the experimental setup employed to assess T cell cytotoxicity elicited in vivo by OMPs. HLA-A2-DR1 mice were vaccinated with OMPs and challenged post-vaccination with syngeneic splenocytes labeled with cell tracking dye. Target T cells (red) were pulsed with a pool of OMPs or TAA-derived peptides and mixed at an equal ratio with unpulsed control cells (black) before being adaptively transferred to immunized mice. (B, C) In vivo cytotoxic activity of OMP-induced T cells against OMP-pulsed or TAAp-pulsed target T cells. Percentages of in vivo specific lysis of splenocytes pulsed with the indicated pool of OMPs (B) or TAA-derived peptide counterparts (C) (challenging peptides) after immunization with the indicated peptide pool or control peptides (immunizing peptides). Data shown in (B) and (C) are from two to four independent experiments, symbols indicate individual mice (n=10–20 mice) and bars represent min and max values. Statistical comparisons were performed using an unpaired non-parametric test (Mann-Whitney). ***p<0.001, ****p<0.0001. (D) Flow cytometry analysis performed on SARC-A2 GFP (left panel) and on SARC-A2-GFP-CD20 (right panel) sarcoma cells showing post-transduction expressions of GFP and hCD20 proteins. (E) Schematic representation of the experimental setup used to evaluate the antitumor effect of OMPs. Mice were immunized with OMP72 using a prime-boost administration regimen. 21 days post-prime immunization, mice were inoculated with hCD20-GFP-expressing or GFP-expressing SARC-A2 sarcoma cells and tumor growth was monitored. (F) Tumor kinetics on individual mice over time for each group. Tumor size in A2/DR1 naïve or OMP vaccinated mice engrafted with 0.5×10^6 SARC-A2-hCD20-GFP or SARC-A2-GFP tumor cells (n=8 mice) was measured (mm^2) over 30 days. (G) hCD20 expression assessment in the vaccinated group. Flow cytometry dot plots showing the expression of human CD20 and GFP in SARC-A2 cells extracted from whole tumors on day 30 in animals still bearing tumors (n=4). (H) Vaccine-specific induced T cell responses. The frequency of peptide-specific T cells producing IFN-γ per million splenic T cells was determined by ELISpot on day 30. ELISpot, Enzyme-Linked ImmunoSpot; HLA, human leukocyte antigen; OMP, OncoMimics peptide; TAAp, tumor-associated antigen-derived peptide.

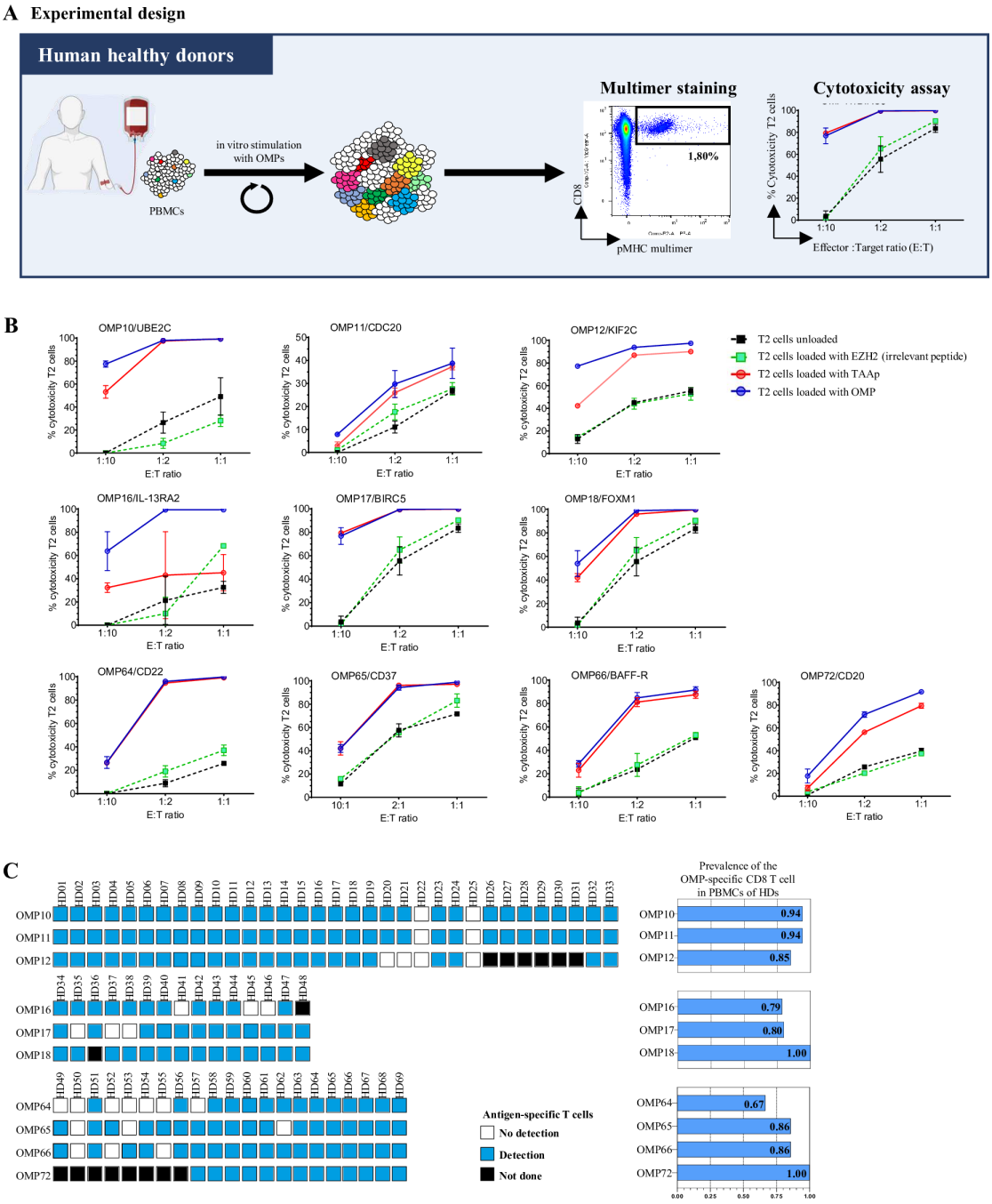

Figure 4 OMP-specific human T cells recognize TAAs and exert specific cytotoxic activity. (A) Schematic overview for determining antigen-specific CD8$^+$ T cell response using healthy volunteer PBMCs and in vitro expansion of CD8$^+$ T cells as described in Material and Methods. (B) Cytotoxic activity of the OMP-specific human CD8$^+$ T cell. CTL killing activity was assessed against T2 cells loaded with OMP and the TAA-derived peptide (TAAp) counterpart after 24 hours incubation. Each graph displays the representative data from healthy donors. The cytotoxicity percentage (y-axis) and effector-to-target ratio (E:T ratio) (x-axis) are indicated on the graph. EZH2-B2 irrelevant peptide and unpulsed T2 cells were used as negative controls. Error bars represent the mean±SD. Solid lines depict T2 cells loaded with bacterial peptides (OMPs in blue) and tumor-associated derived peptides (TAAp in red) and dashed lines represent controls (unloaded in black, EZH2-loaded in green). The cytotoxicity percentage was calculated as specified in the Materials and Methods section. (C) Prevalence of OMP-specific CD8$^+$ T cells in healthy donors (HD). The prevalence of OMP-specific CD8$^+$ T cells in HDs was determined by surface staining using pMHC tetramers after expansion of PBMCs using OMPs and is shown as a histogram. The left panel shows the individual detection of OMPs in each HD, with white, blue and black squares representing HDs in which OMPs were not detected, detected, or no analyses were performed, respectively. The right panel shows the general frequency of OMP detection in healthy donors. The number of analyzed HDs is indicated in parentheses for each OMP: OMP10 and OMP11 (n=33), OMP12 (n=27), OMP16 (n=14), OMP17 (n=15), OMP18 (n=14), OMP64, OMP65, OMP66 (n=21) and OMP72 (n=13). CTL, cytotoxic T cells; OMP, OncoMimics peptide; PBMCs, peripheral blood mononuclear cells; pMHC, peptide major histocompatibility complex; TAA, tumor-associated antigen.

and UCP2, administered in combination with nivolumab (online supplemental figure 4A). Here, we present data from the first three patients included in Cohort 1 (multiple doses of EO2401 monotherapy followed by continued EO2401 in combination with nivolumab), designed to evaluate the safety and tolerability of the approach. Immune responses were evaluated in cryopreserved PBMCs both ex vivo and following IVS. Peptide/MHC tetramer staining, intracellular cytokine staining (ICS) and IFN-γ ELISpot assays were performed.

We initially evaluated the functional capacity and cross-reactivity of OMP-induced T cells following EO2401 treatment using short-term IVS with OMPs followed by tetramer staining. This experimental setup mainly recalls antigen-specific memory and effector T cells, enabling detailed functional analysis.[30] Tetramer staining revealed the presence of OMP-specific T cells for the three OMPs at various frequencies among the patients. EO2317 and EO2318 were the most immunogenic peptides, with significant amplified T cell levels in all three patients. We observed at the plateau of the response (6 weeks) a marked proliferative capacity of OMP-specific T cells at approximately 80%, 35% and 28% of the total $CD8^+$ T cells in Patients #1, #2 and #3, respectively (figure 5A, gating strategy and representative staining in online supplemental figure 4B,C). Long-term follow-up of Patients #1 and #2 revealed a sustained strong immune response until week 44 (figure 5A). Interestingly, we identified in Patients #2 and #3, a pre-existing OMP-specific CD8+T cell population detected on IVS with OMPs before treatment. This population rapidly and strongly increased on EO2401 treatment (figure 5B, online supplemental figure 4C). In the three patients, BIRC5-specific and FOXM1-specific CD8+T cells were observed quickly on EO2401 treatment when T cells were amplified with OMP peptides. In contrast, IL-13RA2-specific T cells were detected at low frequencies in Patient #1 and were below the detection limit in the others (figure 5C and representative staining in online supplemental figure 4D). At the plateau, we observed 40% and 14% BIRC5-specific $CD8^+$ T cells and approximately 1% FOXM1-specific CD8+T cells in patients #1 and #2, respectively. Long-lasting and robust immune responses against BIRC5 and FOXM1 followed the same kinetics as the EO2317-specific and EO2318-specific responses, respectively (figure 5A and C). Only Patient #2 presented a pre-existing BIRC5-specific CD8+T cell population detected on IVS with OMPs, which rapidly and strongly increased on EO2401 treatment (figure 5D, online supplemental figure 4D). We then assessed OMP-specific/TAAp-specific T-cell cross-reactivity by performing tetramer staining on post-IVS PBMCs using the tetramer pairs EO2317/BIRC5 and EO2318/FOXM1 simultaneously. Remarkably, all TAAp-specific $CD8^+$ T cells in the tested patients (Patients #1 and #3) were also labeled to the corresponding OMP tetramer (online supplemental figure 4E). Taken together, we conclude that peptide vaccination with OMPs (EO23016, EO2317 and EO2318) can efficiently mount a rapid and strong OMP-specific T cell response, with high proliferative capacity when re-exposed to OMPs in vitro and cross-reactive capacity to the targeted TAAps (BIRC5, FOXM1 and to a lesser extent, IL-13RA2). Interestingly, in Patient #1, only IVS using OMPs led to the detection of TAAp-specific T cells. When TAAps were used instead of OMPs, we could not detect TAAp-specific T cells independently of peptide concentrations or cytokine conditions. (online supplemental figure 4F,G). TAAp-specific T-cell responses observed after EO2401 treatment can recognize both OMPs and TAAps, but cannot be amplified in vitro with TAAps, suggesting the superior stimulatory capacity of OMPs.

Next, we functionally characterized these OMP/TAAp-specific cross-reactive $CD8^+$ T cells. We used two functional assays (IFN-γ ELISpot and ICS) following IVS with OMPs. High levels of IFN-γ T cell responses against the three OMPs and the TAAp pool were detected in Patients #1 and #2 and, to a lesser extent, in Patient #3. (figure 5E,F). The functionality of these OMP-specific/TAAp-specific $CD8^+$ T cells was confirmed by evaluating the production of Tc1 cytokines (IFN-γ and TNF-α), a Lamp1/CD107a CTL marker and cell activation/proliferation markers (IL-2 and CD154). OMP-polyfunctional and TAA-polyfunctional IFN-γ^+, TNF-α^+, IL-2^+, $CD154^+$ and $CD107a^+$ specific $CD8^+$ T cell responses were observed. Consistent with our previous observations, stronger cytokine levels were observed after restimulation with EO2316, EO2317, EO2318, BIRC5 and to a lesser extent, FOXM1 (figure 5G and representative staining in online supplemental figure 4H).

Based on the high levels of T cells observed after IVS, which suggest either a high proliferative capacity and/or elevated circulating levels of antigen-specific T cells, we investigated these responses directly ex vivo. A significant number of EO2317-specific and EO2318-specific $CD8^+$ T cells were detected ex vivo using MHC tetramers in three patients, with Patient #1 showing 4.7% and 2.7% of EO2317-specific and EO2318-specific $CD8^+$ T cells, respectively. EO2316-specific $CD8^+$ T cells were detected only in Patients #1 and #3 (figure 5H, gating strategy and representative staining: online supplemental figure 4I,J). TAAp-specific T cells were also investigated in Patients #1 and #2. BIRC5-specific $CD8^+$ T cells were detected in both patients, reaching 3.3% in Patient #1. FOXM1-specific $CD8^+$ T cells were detected only in Patient #1, whereas IL-13RA2-specific $CD8^+$ T cells were not detectable ex vivo (figure 5I). The potent proliferative capacity of these OMP-specific/TAAp-specific T cells was underscored when we plotted the number of specific cells obtained ex vivo and the corresponding level after IVS for Patient #1 (figure 5J). These findings indicate both the high circulating levels and high proliferative capacity of antigen-specific T cells induced by EO2401 treatment. We further evaluated the phenotypes of these OMP-specific/TAAp-specific $CD8^+$ T cells in Patients #1 and #2. We demonstrated that the majority (>90%) of these cells exhibited a memory phenotype (T_{EM} and T_{EMRA}) and were functional,

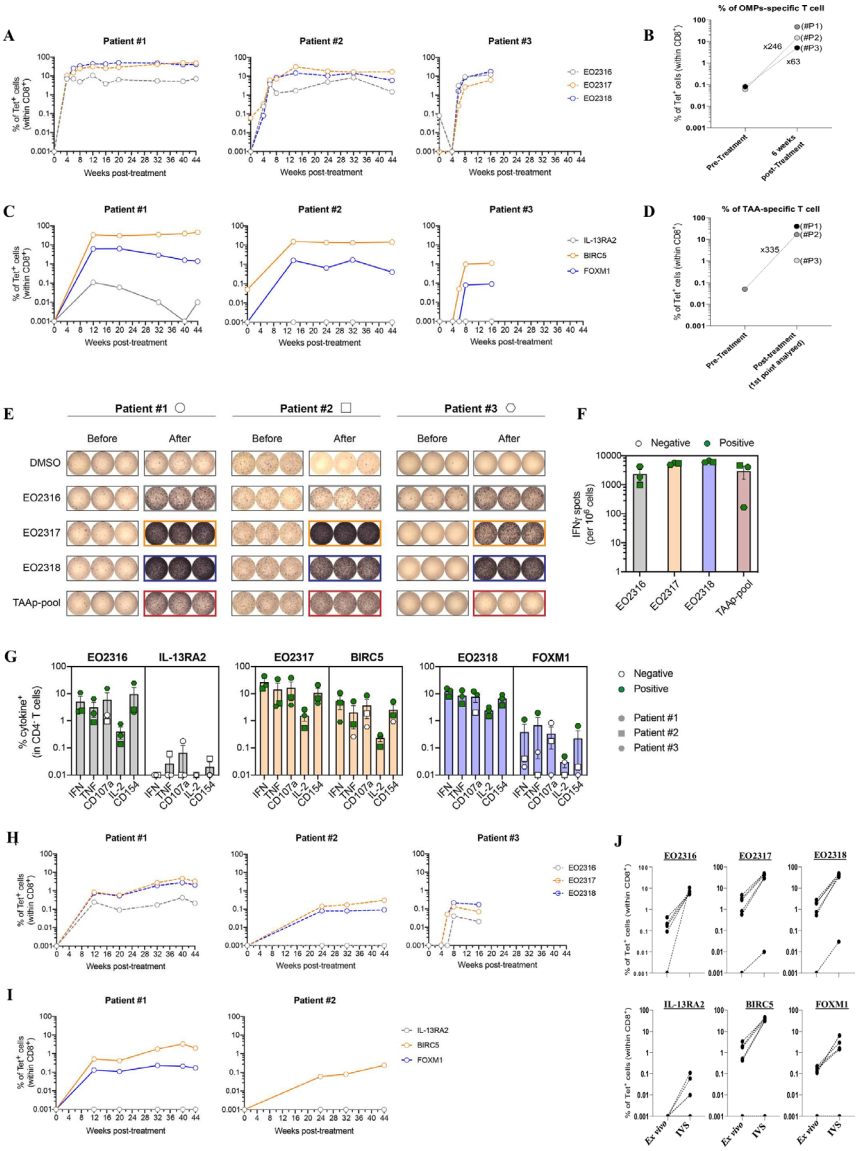

Figure 5 Induction of OMP-specific and TAA-cross-reactive T cell responses in patients with glioblastoma post-vaccination Post-IVS T cell responses to OMPs or TAAps from patients are shown in A–D. (A, C) OMP-specific (A) and TAA-specific (C) CD8$^+$ cells detected using EO2316, EO2317, EO2318, IL-13RA2, BIRC5 and FOXM1 tetramers on PBMC samples subjected to 12 days in vitro stimulation (IVS) with the OMP peptide pool. Data were obtained from all available samples of patients in Cohort 1 (n=3). Each dot represents the percentage of tetramer-positive CD8$^+$ cells in each patient during the defined week. Negative values are plotted at 0.001. (B, D) Immune responses of patients before and after treatment. Total OMP-specific (B) and TAAp-specific (D) CD8$^+$ T cells were detected in patient PBMC samples before and after treatment at the indicated time points. Data represent the added percentages (%) of all OMP (B) or TAAp (D), determined by multimer staining, as shown in (A) and (C). A fold increase was calculated and is shown in the graph when OMPs-specific or TAAp-specific T-cells were detected before treatment. (E–F) Generation of functional antigen-specific cells after vaccination. The immune responses of the patients before and after treatment were analyzed using IFN-γ ELISpot post-IVS. IFN-γ ELISpot wells are shown for all three patients before and after vaccination, with positive wells highlighted with colored squares (E) Quantification of the number of spots after vaccination for each patient, as well as the mean±SEM, are shown in (F). The IFN-γ spots were normalized to 10^6 cells after background subtraction (negative control, DMSO). (G) Polyfunctional T cells are generated by OMP vaccination. ICS quantification of the % of activation marker (IFN-γ, TNF, CD107a, IL-2 and CD154)-positive T-cells on stimulation with the indicated peptides (top of each bar graph). For (F) and (G), Patients #1, #2 and #3 are shown as circles, squares and hexagons, respectively. The symbols filled in green and white represent positive and negative responses, respectively (see Materials and Methods for the positivity criteria). (H–I) (H) OMP-specific CD8$^+$ cells detected using EO2316, EO2317 and EO2318 specific tetramers and (I) TAAp-specific CD8$^+$ cells detected using IL-13RA2, BIRC5 and FOXM1 tetramers in PBMC samples ex vivo. No TAAp-specific data were available for Patient #3. Each dot represents the percentage of tetramer$^+$ CD8$^+$ cells in each patient at the indicated week. Negative values are plotted at 0.001. For Patients #1 and #2, only data from the monitoring of the later time points (12–24 weeks) were available. (J) OMP-specific (top) and TAAp-specific (bottom) CD8$^+$ cells in PBMC ex vivo or after IVS. DMSO, Dimethyl Sulfoxide; ICS, intracellular cytokine staining; OMP, OncoMimics peptide; PBMCs, peripheral blood mononuclear cells; TAA, tumor-associated antigen; TAAp, TAA-derived peptide.

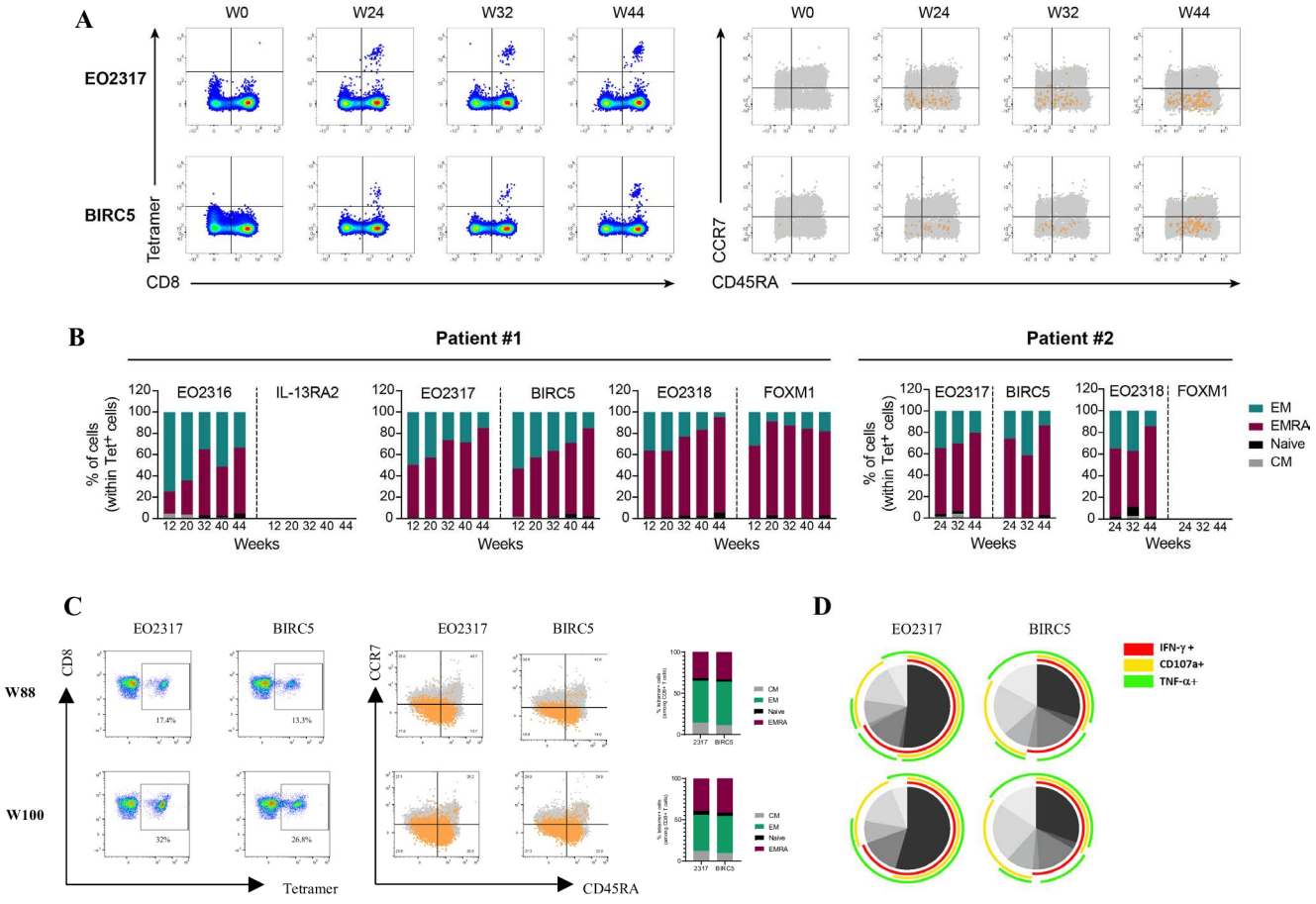

Figure 6 Long-term memory and polyfunctional T cell responses in patients with post-vaccination glioblastoma. (A–B) Vaccine-specific CD8$^+$ T cells are effector memory cells. Representative dot plots (A) for Patient #2 of EO2317-specific and BIRC5-specific CD8$^+$ T cells over time (weeks (W) 0, (W24, W32 and W44) based on tetramer staining (left). The memory phenotype (right) was evaluated based on the expression of the CCR7 and CD45RA markers. CCR7 and CD45RA expression profiles of tetramer$^+$ cells (orange dots) overlaid on CD14/CD19—cells (gray dots). (B) Differentiation of subsets of tetramers+CD8$^+$ T cells. Quantification of the memory phenotype of tetramer$^+$ CD8$^+$ T cells (central memory (CM), naïve, effector memory (EM) and terminally differentiated effector memory (EMRA)) for Patients #1 and #2 is shown as percentages (%). Only the time points with more than 20 tetramer+CD8+ T cells were used for the analysis. (C–D) Durable and long-term responses of Patient #1 to vaccination. T cells from Patient #1 were analyzed at weeks 88 and 100 after administration of the first vaccine dose. Flow cytometry analysis (C) showing EO2317-specific and BIRC5-specific T cells (left) and the CCR7/CD45RA expression profile (middle) for EO2317-specific and BIRC5-specific T cells (orange) overlaid with the overall CD8$^+$ T cell population (gray population). Central memory, effector memory, naïve and terminally differentiated effector memory CD8$^+$ subsets were quantified for each indicated tetramer$^+$ population (right). T cell polyfunctionality is shown in the pie chart (D). T cells were expanded in culture with the OMP pool and IL-2 for 12 days and restimulated with either EO2317 or BIRC5 peptide for 6 hour before being intracellularly stained for IFN-γ, CD107a and TNF-α. The pie arcs depict the proportion of cells that produce a specific cytokine and the pie slices the proportion of cells co-producing one to three different cytokines. Pie arc overlap represents polyfunctional cells.

producing IFN-γ on restimulation with individual OMPs or TAAps tested as a pool (figure 6A,B, online supplemental figure 4K,L).

Our clinical protocol included monthly recall injections, which could potentially lead to alterations in T-cell functionality. To evaluate whether our approach can sustain a robust T-cell response over an extended period, we followed the circulating levels of EO2317-specific/BIRC5-specific T cells in Patient #1 at weeks 88 and 100 ex vivo. At week 44, EO2317 Tetramer$^+$ T cells accounted for 3.27% of the total circulating CD8$^+$ T cells, while BIRC5 Tetramer$^+$ T cells for 1.99% (figure 5H,I). By week 88, the percentage continued to increase to 17.4% for EO2317 Tetramer$^+$ T cells and 13.3% for BIRC5 Tetramer$^+$ T cells. By week 100, these values reached 32% for EO2317 Tetramer$^+$ T cells and 26.8% for BIRC5 Tetramer$^+$ T cells (figure 6C). Interestingly, these long-term cross-reactive EO2317-specific/BIRC5-specific CD8+T cells also maintained a memory phenotype and polyfunctionality (figure 6C,D). These cells were able to produce, for a large majority of them, IFN-γ, TNF-α and CD107a simultaneously on restimulation ex vivo with EO2317 or BIRC5 peptides. This indicates a sustained specific T cell response over time, with these T cells maintaining a polyfunctional and memory phenotype, critical parameters for effective antitumor activity and long-term immune

surveillance. Finally, we evaluated on these patients the ability of the TAAp-specific T cells induced by OMP vaccination to recognize and kill glioblastoma cells in an HLA-A2-restricted context. TAAp-specific T cells were isolated after IVS with the OMPs (EO2316, EO2317 and EO2318) and TAAp-tetramers sorting (figure 7A). FACS analysis confirmed the presence of TAAp-specific T cells in the cell cultures after IVS (figure 7B, left panel). IL13RA2-specific clones were only detected and isolated in patient#1. Following cell sorting and αCD3/CD28 amplification, FACS analysis showed the frequencies of TAAp-specific T cell populations in each individual sorted culture before the cytotoxicity assay (figure 7B, right panel). Individual sorted TAAp-specific T cells from each patient were then tested for their cytotoxic activity against two glioblastoma cell lines (U87 and U118), both naturally expressing IL13RA2, BIRC5 and FOXM1. These TAAp-specific T cells exhibited specific cytotoxic activity against U87 which expresses HLA-A2 but not against U118, an HLA-A2 negative cell line (figure 7C). To confirm the OMP specificity of the sorted TAAp-specific T cells, we performed a cytotoxic assay using T2 cells loaded with the corresponding OMPs. As expected, IL13RA2-Tetramer+T cells specifically killed EO2316-loaded T2 cells, BIRC5-Tetramer+T cells specifically killed EO2317-loaded T2 cells and FOXM1-Tetramer+T cells specifically killed EO2318-loaded T2 cells (online supplemental figure 4M). These findings provide robust evidence that OMP vaccine-induced TAAp-specific $CD8^+$ T cells can effectively recognize and kill tumor cells presenting naturally processed TAAs in an HLA-A2-restricted manner.

DISCUSSION

In this study, we demonstrated that OMPs with a certain degree of sequence homology to TAAps can generate strong and durable cross-reactive T-cell responses against tumor cells. The efficacy of peptide-based immunotherapies relies, in large part, on the properties of the peptides used to activate the immune response against tumor cells. Ideally, these peptides should be highly immunogenic, tumor-specific and activate a T cell population that is prevalent in all patients with cancer. Recent studies have indicated that among patients who undergo ICI administration or neoantigen vaccination, long-term survivors harbor tumor-specific T cells with predicted cross-reactivity to pathogenic bacteria or viral antigens, suggesting that molecular mimicry, T cell cross-reactivity and pre-existing immunity could be key factors for the success of such immunotherapies and, by extension, could be used to improve peptide-based immunotherapies. Extending these findings, it has also been suggested that the composition of the gut microbiome can affect the outcomes of checkpoint blockade therapy.[8 31 32] The human microbiome encodes billions of potential antigens, which is significantly higher than the entire repertoire of known pathogen-derived antigens. Thus, the probability of identifying human mimics of TAAps with the properties set here (figure 1) is certainly high.

For many years, cancer immunotherapies have attempted to leverage TCR cross-reactivity to improve antitumor CTL responses. Altered peptide ligands (APLs), described in the 1990s, were developed to modulate T cell responses through precise modification of peptide sequences.[33 34] Pioneering studies demonstrated that single aa substitutions could modulate T cell activation with effects ranging from superagonism to partial agonism or even antagonism of native peptides.[35–37] These diverse impacts on T cell function have been explored extensively in CD4+T cells, particularly in the context of autoimmune disorders, and several reports suggest that similar mechanisms may apply to CD8+T cells as well.[38–40] Heteroclitic peptides, a subset of APLs, were selected to achieve enhanced immunogenicity and antigenicity through aa substitutions that improve peptide-MHC binding affinity and/or optimize TCR recognition.[41 42] However, despite the strong preclinical efficacy observed with heteroclitic peptides and other APLs, they have not consistently translated into effective cancer vaccines.[43–45] This gap highlights the complexity of immune modulation and the need to refine strategies to fully leverage the potential of T cell cross-reactivity. Given that CDPs naturally shape the T cell repertoire, leveraging their inherent immunogenicity offers a more direct and promising strategy. Our strategy selectively targets OMPs that exhibit improved MHC binding, due to aa mismatches, while preserving the integrity of central TCR contact points to ensure that the TCR can recognize both the OMP and the corresponding TAAp. This finding aligns with recent findings indicating that microbiota-derived peptides with altered TCR contacts may be less effective in triggering cross-reactive CD8 T cells and generating impactful cross-reactive neoantigen CD8 T cells in patients with glioblastoma.[46 47] The T cell repertoire of each individual is shaped by the HLA haplotype and autoantigens encountered during thymic selection. This repertoire is also influenced by various environmental factors, including gut microbiota, which might prime naive T cells and generate a pool of memory T cells.[48 49] The OncoMimics approach was designed to engage this pre-existing T-cell pool. Essentially, if tumor cells present TAAps that sufficiently resemble CDPs, such peptides can be used to reactivate a T-cell pool that cross-reacts with TAAps, potentially leading to tumor control.

OMPs were selected using a bioinformatics pipeline based on the identification of CDPs that share sequence similarities with known TAAps. The selection process involved a Basic Local Alignment Search Tool (BLAST) search that tolerated mismatches at anchor positions and then selected predicted peptides with high HLA-A2 affinity, efficient predicted cleavage and high prevalence of these OMPs within the human microbiome. This approach yielded a list of 4403 OMPs with anticipated high-affinity and cross-reactivity potential. Among the OMP candidates homologous to the analyzed TAAps,

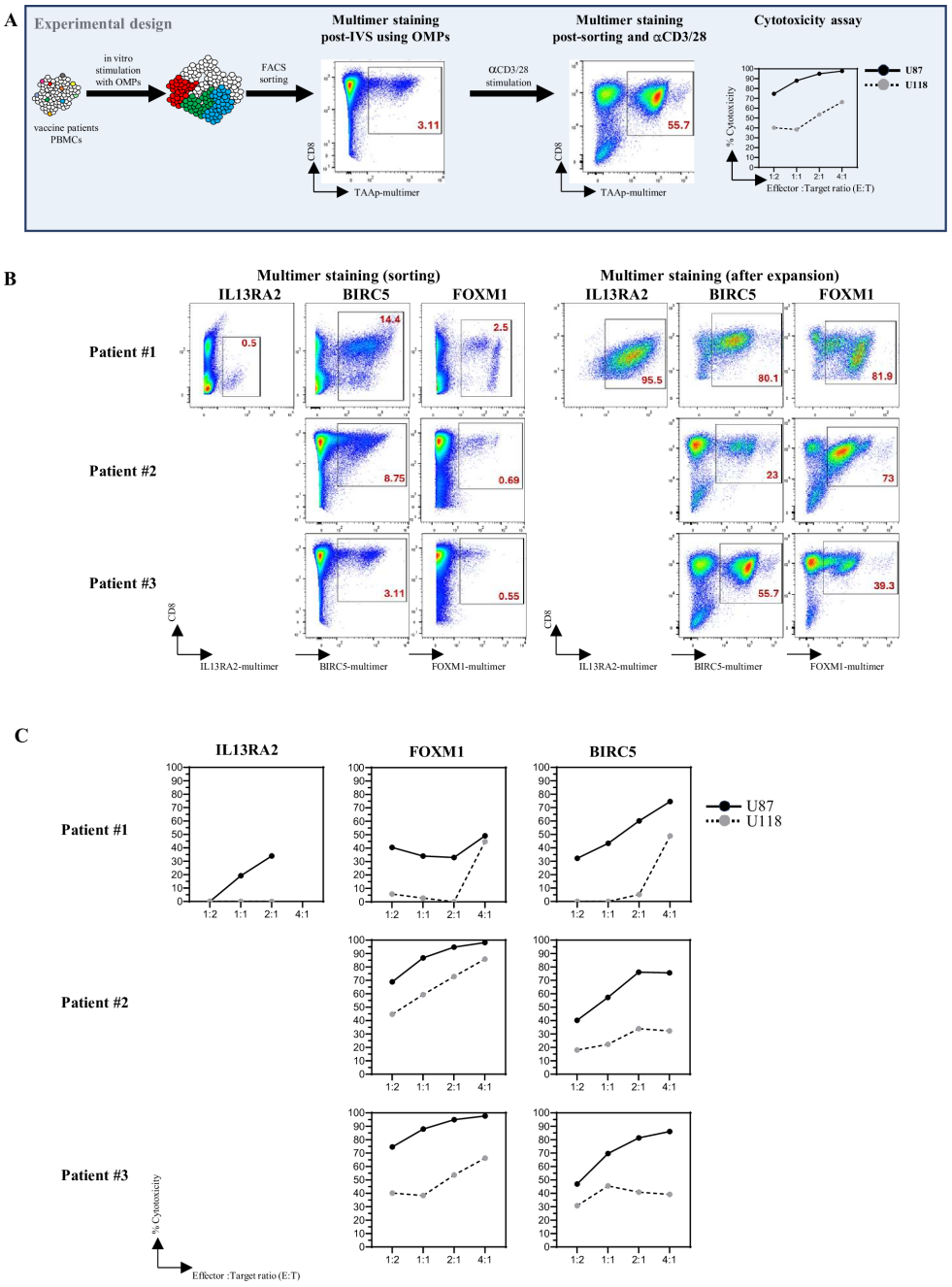

Figure 7 Glioblastoma cell killing by OMP-Induced TAAp-specific T cells in an HLA-restricted manner. (A) Experimental workflow for assessing OMP-Induced TAAp-specific T cell cytotoxicity. PBMCs from vaccinated patients (Patient #1 and #2 V15/week28 and Patient #3 V6/week10) were subjected to IVS with OMPs (EO2316, EO2317 and EO2318) followed by FACS analysis to evaluate the presence of TAAp-specific T cells post-IVS. Subsequently, IL13RA2-specific, BIRC5-specific, and FOXM1-specific T cells were isolated using TAAp-tetramers, expanded for several days with αCD3/CD28 stimulation and analyzed again by FACS to determine the frequencies of TAAp-specific T cells in the culture before proceeding to the cytotoxic assay. (B) FACS analysis of TAAp-specific T cells post-IVS using OMPs and post-sorting and αCD3/CD28 amplification. Left panel: TAAp-Tetramer staining showing the percentage of IL13RA2-specific, BIRC5-specific and FOXM1-specific T cells after IVS using OMPs. Right panel: TAAp-Tetramer staining showing the percentage of IL13RA2-specific, BIRC5-specific and FOXM1-specific T cells after tetramer sorting and αCD3/CD28 amplified in the individual cell cultures from the three patients. (C) Cytotoxic activity of sorted TAA-specific T cells against glioblastoma cells. IL13RA2-specific, BIRC5-specific and FOXM-specific T cells were tested for their killing activity against U87 (HLA-A2$^+$, IL13RA2$^+$, BIRC5$^+$ and FOXM1$^+$) and U118 (HLA-A2$^-$, IL13RA2$^+$, BIRC5$^+$ and FOXM1$^+$) glioblastoma cell lines using various E:T ratios. Cytotoxicity percentages (y-axis) and E:T ratios (x-axis) are shown. The plain lines and closed dark circles indicate U87 cells, while the dotted lines and gray close circles indicate U118 cells. Each point represents the mean of biological duplicates. Cytotoxicity was calculated as specified in the Materials and Methods section. IL13RA2-specific clones were only detected and isolated in patient#1. FACS, Fluorescence-Activated Cell Sorting; HLA, human leukocyte antigen; IVS, in vitro stimulation; OMP, OncoMimics peptide; PBMCs, peripheral blood mononuclear cells; TAAp, tumor-associated antigen -derived peptide.

those with the best scores for binding, cleavage and prevalence were selected. The database we used was derived from the Integrated Gene Catalog, which includes data from 1,267 individuals across Europe, Asia, and North America. However, it under-represents populations from Africa, South America, and other regions, potentially limiting the applicability of OMP panels in these populations. Interestingly, all these OMPs possessed higher HLA-A2-binding affinities and better peptide-MHC stability than their TAAp counterparts, positioning them as suitable candidates to drive strong CTL responses.

Previous research has shown that commensal peptides homologous to tumor antigens can induce cross-reactive T-cell responses critical for tumor control, supporting the hypothesis that microbiota-derived mimic peptides play a significant role in antitumor immunity. For instance, it has been demonstrated that peptides derived from the tail length tape measure protein from Enterococcus hirae can elicit CD8+T cell responses targeting homologous TAAp from the PSMB4 tumor antigen. This cross-reactivity not only enhanced tumor control during immunotherapy in mouse models but also correlated with favorable outcomes in patients with cancer undergoing PD-1 blockade.[48] Similarly, Bifidobacterium breve was shown to express the SVYRYYGL peptide, which mimics the neoantigen SIYRYYGL found in the B16 tumor model. Mice lacking B. breve exhibited reduced neoantigen-reactive T cells and accelerated tumor growth, underscoring that microbial mimicry can stimulate tumor-reactive T-cell responses.[50] More recently, Tripodi *et al* reported that molecular mimicry between Bifidobacterium-derived peptides and melanoma-associated antigens can enhance the efficacy of oncolytic virotherapy by activating cross-reactive T cells. This led to improved tumor control in a syngeneic mouse model of melanoma.[51] While these prior studies underscore the importance of microbiota interactions in cancer therapy, they did not investigate the direct use of microbiota-derived peptides as immunogenic agents to induce cross-reactive T cells. Our study directly addresses this gap. OMPs immune potential was assessed using an A2-DR1 humanized animal model. In this setting, although most OMPs induced stronger TAAp-specific T-cell responses than the TAAps themselves, a few exceptions were noted. For instance, immunogenic responses to CD22 and FOXM1 were lower when OMPs were administered. This can be attributed to the inherent limitations of this model. Specifically, the potential perception of these human TAAps as foreign peptides, due to aa variations with the endogenous mouse equivalent (online supplemental table 3) and the absence of these human OMPs in mouse gut microbiota, could skew a biased T cell repertoire. Such factors potentially limit our model from fully recapitulating human immune responses. The A2/DR1 murine model provided a valuable model system for evaluating the potential of OMPs to induce cross-reactive T-cell responses. However, differences in microbiota composition and immune repertoire between mice and humans highlight the need for a cautious interpretation of our comparative immunogenicity results between the OMPs and TAAps. Importantly, we explored the capacity of OMPs to trigger a functional CTL response to TAAps in vivo. We observed that OMPs were able to induce cross-reactive OMP-/TAAp-specific T cells that could recognize and kill TAAp-loaded target cells. Additionally, we also confirmed that OMP72-specific/CD20-specific T-cell responses triggered by OMP72 could induce protection against CD20-expressing tumor cells in a tumor protection model. While these findings highlight the potential of OMPs to elicit functional antitumor immune responses, a therapeutic model would have been an ideal extension to evaluate their therapeutic potential. Unfortunately, the inherent limitations of the available syngeneic tumor models in HLA-A2/DR1 mice precluded such studies. The development of additional tumor models with stable TAA expression and lower immunogenicity will be critical for future preclinical studies. Our findings align with previous reports in wild-type (WT) mouse models, where viral-derived peptides similar to tumor peptides to provoke cross-reactive T-cell responses. For example, viral-derived peptides homologous to tumor antigens have demonstrated the ability to prime pre-existing cross-reactive T cells through direct peptide vaccination, effectively targeting tumors presenting the corresponding TAAp.[52 53] These approaches address the low immunogenicity of natural tumor antigens and leverage pre-existing memory T cell priming by past infections. The success of pathogen-mimicking strategies is inherently limited by the individual pathogen exposure histories of each patient, complicating the development of universally effective treatments. In contrast, our investigation of the widespread presence of OMP-specific T cells in the human population revealed that more than 80% of the tested HD PBMCs (8 of 10 OMPs) contained such T cell pools. Furthermore, PBMCs expanded with OMPs in vitro demonstrated cross-reactivity and specific CTL activity against tumor cells presenting both peptides, even at low E:T ratios. This finding supports the potential of OMPs for developing broadly applicable peptide-based immunotherapeutic strategies in humans. Based on these findings, specific OMPs have been used to develop off-the-shelf peptide-based immunotherapy that is currently undergoing clinical evaluation. EO2401 peptide-based immunotherapy includes three OMPs (EO2316/OMP16, EO2317/OMP17 and EO2318/OMP18) that mimic TAAps (IL-13RA2, BIRC5 and FOXM1) and is currently being evaluated in a multicenter phase Ib/IIa clinical trial (EOGBM1-18, NCT04116658) in patients with recurrent glioblastoma. The selection of IL-13RA2, BIRC5 and FOXM1 as targets for patients with Glioblastoma (GBM) using our approach is supported by scientific and clinical data validating their expression in GBM tumors, as well as the presentation of the targeted TAAps by tumor cells.[54–56] Initial immunomonitoring data obtained from blood samples of three patients included in the first cohort demonstrated that this approach is unique among other

peptide-based therapies in its ability to generate robust CD8+T cell responses. Specifically, a strong immune response against OMPs and targeted TAAps was induced in all three patients, with ex vivo frequencies of TAAp-specific circulating T cells exceeding 1% of total CD8+T cells. In these patients, we observed distinct patterns of immune responses among the OMP/TAAp pairs: EO2317 and EO2318 elicited higher levels of cross-reactive BIRC5-specific and FOXM1-specific T-cell responses, respectively 80% of EO2317-specific T cells also recognized BIRC5-specific and around 20% of EO2318-specific T cells were also FOXM1-specific. In contrast, EO2316 demonstrated a lower capacity to trigger cross-reactive EO2316-/IL-13RA2-specific T cells with just 1% of EO2316-specific T cells cross-reacting with IL13RA2. Therefore, the effectiveness of each OMP/TAAp pair is determined by factors beyond peptide-MHC binding affinity. Notably, intrinsic TCR cross-reactivity rules for each peptide pair and variations in individual gut microbiota compositions could significantly influence their effectiveness. Ongoing analysis of the stool samples collected from patients before and after vaccination will definitively assess the precise relationship between the gut microbiota and the OMPs bacteria of origin. This analysis will assess key parameters, including the specific taxa expressing the OMPs, their expression levels, gut localization, and protein of origin (eg, secreted, cytosolic, membrane-bound) and examine the impact of these microbial factors on the strength and persistence of OMP-induced T-cell responses and their correlation with clinical outcomes, interestingly, for Patient #1, the administration of EO2317 led to an impressive expansion of BIRC5-specific CD8+T cells, with more than 20% of the total circulating $CD8^+$ T cells. This remarkable expansion surpasses the typical outcomes observed with classical vaccination approaches (0.1–1%), for which the frequency of circulating tumor antigen-specific CD8+T cells is rarely detectable ex vivo by MHC-tetramer.[57] These findings demonstrated robust and sustained responses, with ex vivo T-cell percentages in the single-digit or double-digit range. Importantly, for therapeutic considerations, OMPs elicited persistent tumor antigen-specific T-cell responses in Patient #1, extending for almost 2 years (week 100) of treatment while maintaining their cross-reactivity and polyfunctional properties. Notably, these levels exceed in the long term those reported for Chimeric Antigen Receptor T-cell (CAR-T) or T-Cell Receptor T-cell (TCR-T) therapies, for which the number of cells initially injected rapidly declines over time.[58 59] It remains uncertain whether continued OMP vaccination is necessary to sustain the cross-reactive T cell population or not. In addition, our analysis does not guarantee the complete absence of exhaustion, as some functional properties can persist even in T cells displaying exhaustion markers.[60] Additional investigations using exhaustion markers such as LAG3, TIM3, TIGIT, CD38, CD57 and transcriptional regulators like TOX are necessary to provide a more comprehensive understanding of the functional state of these T cells.

The rapid and sustained immune responses observed in the three patients as early as 4 weeks after the first administration suggest that our approach targets a highly proliferative T-cell population, which we hypothesized to be a pre-existing memory cell population. This observation is reinforced by the level of immune response and the large number of circulating memory T cells (based on CD45RA/CCR7 markers) observed early after vaccination, which demonstrates the robust in vivo expansion of effector memory $CD8^+$ T cells. These observations strongly support the hypothesis that memory T cells activated by OMP vaccination are initially generated through the exposure of gut T cells to commensal peptides. However, it remains to be determined whether these OMP-specific T cells originate from a preprimed gut-derived memory T-cell pool. Interestingly, IVS experiments also demonstrated that OMP-specific/TAAp-specific T cells were expandable when stimulated with OMPs but not with TAAps underscoring their superior ability to stimulate T cell proliferation. This observation aligns with findings using a superagonist MART-1 peptide, which also showed enhanced T cell activation compared with the native peptide in patients with cancer.[61] Functional analysis of these post-IVS T cells showed that they were not only highly proliferative on OMP stimulation but also demonstrated a polyfunctional phenotype on OMP and TAAp restimulation. This indicates that OMPs effectively trigger OMP-specific/TAAp-specific T cells, which can expand on OMP stimulation and remain responsive to both OMP and TAAp activation, highlighting the superior priming activity of OMPs. Our study primarily investigated the efficacy of OMPs in eliciting OMP-specific/TAAp-specific cross-reactive T cells in the peripheral blood. More importantly, we demonstrate that OMP-specific/TAAp-specific T cells obtained from vaccinated patients are cytotoxic against glioblastoma cells presenting naturally processed TAAs. This provides proof of the principle that the OncoMimics vaccine approach can stimulate antitumor T cells in patients with glioblastoma. Consistent with studies showing that tumor-specific T cells can migrate from the peripheral blood and infiltrate brain tumors after peptide-based immunotherapy,[62 63] preliminary data from patient-derived relapsed tissues showed CD8+T cell recruitment within tumors following EO2401 treatment.[64] To conclusively establish the specificity and migration patterns of OMP-/TAAp-induced T cells, further in-depth analyses involving tumour-infiltrating lymphocyte (TIL) isolation and subsequent tetramer staining or single-cell TCR profiling are required. Notably, supporting our approach, a recent study demonstrated that glioblastoma $CD4^+$ TILs can recognize a diverse array of peptides, including peptides derived from the commensal gut microbiota.[65]

In summary, we have shown that commensal bacteria-derived peptides, with homology to naturally occurring TAAps, when carefully chosen through a combined bioinformatic and lab-assay pipeline, can be used to generate rapid and long-lasting immune $CD8^+$ T cell responses at high frequencies. We applied this approach for the

first time to vaccinate patients with glioblastoma, a low mutation-burden tumor for which ICI trials have not shown any clinical benefit. Extremely potent and long-lasting immune responses were observed in the first three patients. Although follow-up is required to confirm these conclusions, we observed that two of the three patients survived beyond 1 year. Although preliminary, this outcome offers a cautiously optimistic perspective in the context of challenging clinical conditions and provides some guidelines for further clinical trials.[66] Our approach focuses on the direct administration of OMPs in combination with a Montanide adjuvant and PD-1 checkpoint blockade. Nevertheless, the incorporation of alternative or complementary strategies may significantly enhance the therapeutic potential of OMP-based immunotherapies.[67] For instance, using OMPs within dendritic cell-based vaccines could amplify antigen presentation and boost immune recognition.[68] Advanced delivery platforms such as nanoparticles, virus-like particles or outer membrane vesicles could on the other hand improve OMP delivery, targeting and immune activation.[69] Additionally, integrating OncoMimics into a messenger RNA-based platform offers a solution to encode multiple OMPs within a single construct addressing a key challenge of peptide solubility, stability and manufacturing costs, while enabling flexible and scalable production. These complementary strategies offer a promising framework for expanding the effectiveness of OMPs, especially when it comes to treating a variety of tumor types and improving patient outcomes.

Author affiliations
[1]Enterome, Paris, Île-de-France, France
[2]Institute for Immunology and Cluster of Excellence iFIT (EXC2180), Image-Guided and Functionally Instructed Tumor Therapies, Eberhard-Karls-University Tübingen, Tübingen, Germany
[3]Toulouse Institute for Infectious and Inflammatory Diseases (Infinity), INSERM UMR1291 – CNRS UMR5051 – University Toulouse III, Toulouse, France
[4]Université de Franche-Comté, EFS, INSERM, UMR 1098 RIGHT, F-25000 Besançon, France
[5]Sorbonne Université, AP-HP, ICM, Hôpital Universitaire La Pitié-Salpêtrière, Paris, France
[6]Hospital Universitari Vall d'Hebron, Barcelona, Catalunya, Spain
[7]UMR 1231, Centre Georges-Francois Leclerc, Dijon, Bourgogne-Franche-Comté, France
[8]Institut Catala D'Oncologia - Hospital Duran i Reynals, Barcelona, Spain
[9]Department of Neurology & Interdisciplinary Neuro-Oncology, University Hospital Tübingen, Hertie Institute for Clinical Brain Research, Center for Neuro-Oncology, Comprehensive Cancer Center, Stuttgart, Germany
[10]Dr. Senckenberg Institute of Neurooncology, Goethe University Hospital, Frankfurt, Germany
[11]Universitat Heidelberg Medizinische Fakultat Mannheim, Mannheim, Baden-Württemberg, Germany
[12]Division of Clinical Neurooncology, Department of Neurology and Center of Integrated Oncology, University Hospital Bonn, Bonn, Nordrhein-Westfalen, Germany
[13]Dana-Farber Cancer Institute, Boston, Massachusetts, USA
[14]Universitätsklinikum Heidelberg and German Cancer Research Center, Heidelberg, Baden-Württemberg, Germany

X Joao Gamelas Magalhaes @JGM_Lab

Acknowledgements We would like to thank the patients and their families who participated in Cohort 1 of the EOGBM1-18 study (NCT04116658). We would like to express our sincere gratitude to Professor Pedro Romero of the University of Lausanne, Professor David Klatzmann, Professor of Immunology at Sorbonne Université and Head of Biotherapy at Pitié-Salpêtrière Hospital for their comments, suggestions and manuscript review. Their expertise significantly advanced and shaped the project. We thank Muriel Mas, Jean-Michel Paillarse and Jan Fagerberg, whose pivotal roles were instrumental in steering the clinical development of this study. We thank all Enterome employees for their dedication that enabled this study. We also thank Rachel Morra and Guillame Bayre for their assistance with editing and proofreading the manuscript. We used the ARRIVE checklist when writing our report.[70] Figures were created using biorender.com software. We thank Barbora Vrablikova, Odile Ruckebusch and Aurélie Guguin from the IMRB cytometry platform for cell sorting.

Contributors JGM, CBo and LC conceived and designed the study; drafted the original manuscript and supervised the project. JGM is the guarantor of the work. AT, AMai, J-MC, GK, OA, OJ, LC and JGM conducted formal analyses. AT, J-MC, AMai, GK, LAu, LAm, JK, TM, AG, CO, CC, DB, CV, LBe, AMan, JM, MB, JN, KL, LBo, MM and JGM performed experiments. CBi, CGa, FS and JGM were responsible for the bioinformatics data curation. AT, J-MC, GK, AMai, LAu, JK, FS and JGM contributed to the methodology development. OA, OJ, CGo, LC and JGM administered the study. AMai, CGo, AI, MV, FG, AS, GT, MCB, IM, UH, WW and DR contributed the resources. AT, J-MC, GK, AMai, LAu, JK, CGo and JGM verified the replication and reproducibility of the results and created the visualization and data presentation. All authors reviewed, edited and approved the final manuscript.

Funding This study was funded by Enterome. ROSALIE/EOGBM1-18 Study (NCT04116658) is sponsored by Enterome.

Competing interests FS, CBo and LC are co-inventors of the international patent application PCT/EP2019/059329 entitled 'Antigenic peptides for the prevention and treatment of cancer'. GK, FS, LC and JGM are co-inventors of the international patent application PCT/EP2020/082101, entitled 'Antigenic peptides for prevention and treatment of B-cell malignancy'. GK, CGa, AT, FS, LC and JGM are co-inventors of the international patent application PCT/EP2023/058415 entitled 'Antigenic peptides for prevention and treatment of cancer'. These patent applications claim the OncoMimics peptides described in this manuscript. Enterome employed AT, J-MC, GK, CGa, FS, CBi, LAu, LAm, JK, TM, AG, CO, CC, DB, CV, LBe, AMan, JM, MB, GC, CBo, LC and JGM at the time of this study. CGo and AMai received funding from Enterome at the time of the study. All other authors declare no competing interests.

Patient consent for publication Not applicable.

Ethics approval Not applicable.

Provenance and peer review Not commissioned; externally peer reviewed.

Data availability statement Data are available upon reasonable request. All data relevant to the study are included in the article or uploaded as supplementary information. Data are available on reasonable request. All relevant data are available in the article or uploaded as online supplemental information. Request for additional information, resources, reagents and unique materials developed in this study should be directed to the corresponding author and subject to a material transfer agreement.

ORCID iDs
Alice Talpin http://orcid.org/0009-0004-4056-1002
Ana Maia http://orcid.org/0000-0003-1261-7211
Jean-Marie Carpier http://orcid.org/0009-0003-7324-2844
Guillaume Kulakowski http://orcid.org/0009-0009-4203-4448
Lucie Aubergeon http://orcid.org/0000-0002-3459-7904
Jerome Kervevan http://orcid.org/0000-0002-5070-022X

Camille Gaal http://orcid.org/0000-0001-7749-4609
Francesco Strozzi http://orcid.org/0000-0002-6845-6982
Coline Billerey http://orcid.org/0009-0008-8924-682X
Ludivine Amable http://orcid.org/0009-0006-4734-0565
Tifanny Mersceman http://orcid.org/0009-0007-2122-0554
Alexandrine Garnier http://orcid.org/0009-0001-9845-1023
Càtia Oliveira http://orcid.org/0009-0009-0001-051X
Carolina Calderon http://orcid.org/0009-0008-8072-1890
Diana Bachrouche http://orcid.org/0009-0008-6817-3625
Chloé Ventujol http://orcid.org/0009-0006-5095-9430
Léa Bernard http://orcid.org/0009-0001-5449-9025
Amandine Manteau http://orcid.org/0009-0005-2257-2872
Jennifer Martinez http://orcid.org/0009-0001-2966-6194
Michaël Bonnet http://orcid.org/0009-0003-7698-5133
Julie Noguerol http://orcid.org/0009-0007-7166-5797
Karl Laviolette http://orcid.org/0009-0002-2940-8336
Laura Boullerot http://orcid.org/0000-0002-2029-4742
Marine Malfroy http://orcid.org/0009-0005-7013-1668
Gregoire Chevalier http://orcid.org/0000-0003-4698-1206
Olivier Adotevi http://orcid.org/0000-0002-7742-136X
Olivier Joffre http://orcid.org/0000-0003-1168-8165
Francois Ghiringhelli http://orcid.org/0000-0002-5465-8305
Cecile Gouttefangeas http://orcid.org/0000-0002-6410-2378
Laurent Chene http://orcid.org/0009-0006-2436-0520
Joao Gamelas Magalhaes http://orcid.org/0000-0003-4667-605X

REFERENCES

1 Vafaei S, Zekiy AO, Khanamir RA, *et al*. Combination therapy with immune checkpoint inhibitors (ICIs); a new frontier. *Cancer Cell Int* 2022;22:2.
2 Lin MJ, Svensson-Arvelund J, Lubitz GS, *et al*. Cancer vaccines: the next immunotherapy frontier. *Nat Cancer* 2022;3:911–26.
3 Fan T, Zhang M, Yang J, *et al*. Therapeutic cancer vaccines: advancements, challenges, and prospects. *Signal Transduct Target Ther* 2023;8:450.
4 Buonaguro L, Tagliamonte M. Selecting Target Antigens for Cancer Vaccine Development. *Vaccines (Basel)* 2020;8:615.
5 Xie N, Shen G, Gao W, *et al*. Neoantigens: promising targets for cancer therapy. *Signal Transduct Target Ther* 2023;8:9.
6 Mason D. A very high level of crossreactivity is an essential feature of the T-cell receptor. *Immunol Today* 1998;19:395–404.
7 Gouttefangeas C, Klein R, Maia A. The good and the bad of T cell cross-reactivity: challenges and opportunities for novel therapeutics in autoimmunity and cancer. *Front Immunol* 2023;14:1212546.
8 Tian J, Ma J. The Value of Microbes in Cancer Neoantigen Immunotherapy. *Pharmaceutics* 2023;15:2138.
9 Tomasi M, Caproni E, Benedet M, *et al*. Outer Membrane Vesicles From The Gut Microbiome Contribute to Tumor Immunity by Eliciting Cross-Reactive T Cells. *Front Oncol* 2022;12:912639.
10 Buonaguro L, Tagliamonte M. Peptide-based vaccine for cancer therapies. *Front Immunol* 2023;14:1210044.
11 Plonquet A, Garcia-Pons F, Fernandez E, *et al*. Peptides derived from the onconeural HuD protein can elicit cytotoxic responses in HHD mouse and human. *J Neuroimmunol* 2003;142:93–100.
12 Pajot A, Michel M-L, Fazilleau N, *et al*. A mouse model of human adaptive immune functions: HLA-A2.1-/HLA-DR1-transgenic H-2 class I-/class II-knockout mice. *Eur J Immunol* 2004;34:3060–9.
13 Wolfl M, Kuball J, Ho WY, *et al*. Activation-induced expression of CD137 permits detection, isolation, and expansion of the full repertoire of CD8+ T cells responding to antigen without requiring knowledge of epitope specificities. *Blood* 2007;110:201–10.
14 Khalaf WS, Garg M, Mohamed YS, *et al*. *In vitro* Generation of Cytotoxic T Cells With Potential for Adoptive Tumor Immunotherapy of Multiple Myeloma. *Front Immunol* 2019;10:1792.
15 Campillo-Davo D, Fujiki F, Van den Bergh JMJ, *et al*. Efficient and Non-genotoxic RNA-Based Engineering of Human T Cells Using Tumor-Specific T Cell Receptors With Minimal TCR Mispairing. *Front Immunol* 2018;9:2503.
16 Schuhmacher J, Kleemann L, Richardson JR, *et al*. Simultaneous Identification of Functional Antigen-Specific CD8+ and CD4+ Cells after In Vitro Expansion Using Elongated Peptides. *Cells* 2022;11:3451.
17 Widenmeyer M, Griesemann H, Stevanović S, *et al*. Promiscuous survivin peptide induces robust CD4+ T-cell responses in the majority of vaccinated cancer patients. *Int J Cancer* 2012;131:140–9.
18 Moodie Z, Price L, Gouttefangeas C, *et al*. Response definition criteria for ELISPOT assays revisited. *Cancer Immunol Immunother* 2010;59:1489–501.
19 Chen KY, Liu J, Ren EC. Structural and functional distinctiveness of HLA-A2 allelic variants. *Immunol Res* 2012;53:182–90.
20 Li J, Jia H, Cai X, *et al*. An integrated catalog of reference genes in the human gut microbiome. *Nat Biotechnol* 2014;32:834–41.
21 Szeto C, Lobos CA, Nguyen AT, *et al*. TCR Recognition of Peptide-MHC-I: Rule Makers and Breakers. *Int J Mol Sci* 2020;22:68.
22 Zeng J, Zhang J, Yang Y-Z, *et al*. IL13RA2 is overexpressed in malignant gliomas and related to clinical outcome of patients. *Am J Transl Res* 2020;12:4702–14.
23 Wheatley SP, Altieri DC. Survivin at a glance. *J Cell Sci* 2019;132:jcs223826.
24 Li L, Wu D, Yu Q, *et al*. Prognostic value of FOXM1 in solid tumors: a systematic review and meta-analysis. *Oncotarget* 2017;8:32298–308.
25 Xie C, Powell C, Yao M, *et al*. Ubiquitin-conjugating enzyme E2C: a potential cancer biomarker. *Int J Biochem Cell Biol* 2014;47:113–7.
26 Gayyed MF, El-Maqsoud NMRA, Tawfiek ER, *et al*. A comprehensive analysis of CDC20 overexpression in common malignant tumors from multiple organs: its correlation with tumor grade and stage. *Tumor Biol* 2016;37:749–62.
27 Zhang X, Li Y, Hu P, *et al*. KIF2C is a Biomarker Correlated With Prognosis and Immunosuppressive Microenvironment in Human Tumors. *Front Genet* 2022;13:891408.
28 Crees ZD, Ghobadi A. Cellular Therapy Updates in B-Cell Lymphoma: The State of the CAR-T. *Cancers (Basel)* 2021;13:5181.
29 Rangan L, Galaine J, Boidot R, *et al*. Identification of a novel PD-L1 positive solid tumor transplantable in HLA-A*0201/DRB1*0101 transgenic mice. *Oncotarget* 2017;8:48959–71.
30 Todryk SM, Pathan AA, Keating S, *et al*. The relationship between human effector and memory T cells measured by ex vivo and cultured ELISPOT following recent and distal priming. *Immunology* 2009;128:83–91.
31 Sioud M. T-cell cross-reactivity may explain the large variation in how cancer patients respond to checkpoint inhibitors. *Scand J Immunol* 2018;87.
32 Leng Q, Tarbe M, Long Q, *et al*. Pre-existing heterologous T-cell immunity and neoantigen immunogenicity. *Clin Transl Immunology* 2020;9:e01111.
33 Evavold BD, Allen PM. Separation of IL-4 production from Th cell proliferation by an altered T cell receptor ligand. *Science* 1991;252:1308–10.
34 Candia M, Kratzer B, Pickl WF. On Peptides and Altered Peptide Ligands: From Origin, Mode of Action and Design to Clinical Application (Immunotherapy). *Int Arch Allergy Immunol* 2016;170:211–33.
35 Madrenas J, Germain RN. Variant TCR ligands: new insights into the molecular basis of antigen-dependent signal transduction and T-cell activation. *Semin Immunol* 1996;8:83–101.
36 Sloan-Lancaster J, Allen PM. Altered peptide ligand-induced partial T cell activation: molecular mechanisms and role in T cell biology. *Annu Rev Immunol* 1996;14:1–27.
37 Ausubel LJ, Krieger JI, Hafler DA. Changes in cytokine secretion induced by altered peptide ligands of myelin basic protein peptide 85-99. *J Immunol* 1997;159:2502–12.
38 Höllsberg P, Weber WE, Dangond F, *et al*. Differential activation of proliferation and cytotoxicity in human T-cell lymphotropic virus type I Tax-specific CD8 T cells by an altered peptide ligand. *Proc Natl Acad Sci U S A* 1995;92:4036–40.
39 Dressel A, Chin JL, Sette A, *et al*. Autoantigen recognition by human CD8 T cell clones: enhanced agonist response induced by altered peptide ligands. *J Immunol* 1997;159:4943–51.
40 Loftus DJ, Squarcina P, Nielsen MB, *et al*. Peptides derived from self-proteins as partial agonists and antagonists of human CD8+ T-cell clones reactive to melanoma/melanocyte epitope MART1(27-35). *Cancer Res* 1998;58:2433–9.
41 Valmori D, Fonteneau JF, Lizana CM, *et al*. Enhanced generation of specific tumor-reactive CTL in vitro by selected Melan-A/MART-1 immunodominant peptide analogues. *J Immunol* 1998;160:1750–8.
42 Rivoltini L, Squarcina P, Loftus DJ, *et al*. A superagonist variant of peptide MART1/Melan A27-35 elicits anti-melanoma CD8+ T cells with enhanced functional characteristics: implication for more effective immunotherapy. *Cancer Res* 1999;59:301–6.
43 Filipazzi P, Pilla L, Mariani L, *et al*. Limited induction of tumor cross-reactive T cells without a measurable clinical benefit in early melanoma patients vaccinated with human leukocyte antigen class I-modified peptides. *Clin Cancer Res* 2012;18:6485–96.
44 Speiser DE, Baumgaertner P, Voelter V, *et al*. Unmodified self antigen triggers human CD8 T cells with stronger tumor reactivity than altered antigen. *Proc Natl Acad Sci U S A* 2008;105:3849–54.

45 Madura F, Rizkallah PJ, Holland CJ, *et al*. Structural basis for ineffective T-cell responses to MHC anchor residue-improved 'heteroclitic' peptides. *Eur J Immunol* 2015;45:584–91.
46 Buonaguro L, Cavalluzzo B, Mauriello A, *et al*. Microorganisms-derived antigens for preventive anti-cancer vaccines. *Mol Aspects Med* 2023;92:101192.
47 Wang J, Weiss T, Neidert MC, *et al*. Vaccination with Designed Neopeptides Induces Intratumoral, Cross-reactive CD4+ T-cell Responses in Glioblastoma. *Clin Cancer Res* 2022;28:5368–82.
48 Fluckiger A, Daillère R, Sassi M, *et al*. Cross-reactivity between tumor MHC class I-restricted antigens and an enterococcal bacteriophage. *Science* 2020;369:936–42.
49 Cavalluzzo B, Viuff MC, Tvingsholm SA, *et al*. Cross-reactive CD8$^+$ T cell responses to tumor-associated antigens (TAAs) and homologous microbiota-derived antigens (MoAs). *J Exp Clin Cancer Res* 2024;43:87.
50 Sivan A, Corrales L, Hubert N, *et al*. Commensal Bifidobacterium promotes antitumor immunity and facilitates anti-PD-L1 efficacy. *Science* 2015;350:1084–9.
51 Tripodi L, Feola S, Granata I, *et al*. Bifidobacterium affects antitumor efficacy of oncolytic adenovirus in a mouse model of melanoma. *iScience* 2023;26:107668.
52 Chiaro J, Kasanen HHE, Whalley T, *et al*. Viral Molecular Mimicry Influences the Antitumor Immune Response in Murine and Human Melanoma. *Cancer Immunol Res* 2021;9:981–93.
53 Ragone C, Manolio C, Cavalluzzo B, *et al*. Identification and validation of viral antigens sharing sequence and structural homology with tumor-associated antigens (TAAs). *J Immunother Cancer* 2021;9:e002694.
54 Okano F, Storkus WJ, Chambers WH, *et al*. Identification of a novel HLA-A*0201-restricted, cytotoxic T lymphocyte epitope in a human glioma-associated antigen, interleukin 13 receptor alpha2 chain. *Clin Cancer Res Off J Am Assoc Cancer Res* 2002;8:2851–5.
55 Ahluwalia MS, Reardon DA, Abad AP, *et al*. Phase IIa Study of SurVaxM Plus Adjuvant Temozolomide for Newly Diagnosed Glioblastoma. *J Clin Oncol* 2023;41:1453–65.
56 Tabnak P, Hasanzade Bashkandi A, Ebrahimnezhad M, *et al*. Forkhead box transcription factors (FOXOs and FOXM1) in glioma: from molecular mechanisms to therapeutics. *Cancer Cell Int* 2023;23:238.
57 Romero P, Cerottini J-C, Speiser DE. Monitoring tumor antigen specific T-cell responses in cancer patients and phase I clinical trials of peptide-based vaccination. *Cancer Immunol Immunother* 2004;53:249–55.
58 López-Cantillo G, Urueña C, Camacho BA, *et al*. CAR-T Cell Performance: How to Improve Their Persistence? *Front Immunol* 2022;13:878209.
59 Greenbaum U, Dumbrava EI, Biter AB, *et al*. Engineered T-cell Receptor T Cells for Cancer Immunotherapy. *Cancer Immunol Res* 2021;9:1252–61.
60 Blank CU, Haining WN, Held W, *et al*. Defining 'T cell exhaustion'. *Nat Rev Immunol* 2019;19:665–74.
61 Galloway SAE, Dolton G, Attaf M, *et al*. Peptide Super-Agonist Enhances T-Cell Responses to Melanoma. *Front Immunol* 2019;10:319.
62 Keskin DB, Anandappa AJ, Sun J, *et al*. Neoantigen vaccine generates intratumoral T cell responses in phase Ib glioblastoma trial. *Nature New Biol* 2019;565:234–9.
63 Hilf N, Kuttruff-Coqui S, Frenzel K, *et al*. Actively personalized vaccination trial for newly diagnosed glioblastoma. *Nature New Biol* 2019;565:240–5.
64 Reardon D, Idbaih A, Vieito M, *et al*. CTIM-25. EO2401 PEPTIDE IMMUNOTHERAPY + NIVOLUMAB +/- BEVACIZUMAB IN FIRST RECURRENT GLIOBLASTOMA: THE PHASE 1/2 EOGBM1-18/ROSALIE STUDY (NCT04116658). *Neuro-oncology* 2023;25:v67–8.
65 Naghavian R, Faigle W, Oldrati P, *et al*. Microbial peptides activate tumour-infiltrating lymphocytes in glioblastoma. *Nature New Biol* 2023;617:807–17.
66 Wick W, Idbaih A, Tabatabai G, *et al*. EO2401, a novel microbiome-derived therapeutic vaccine for patients with recurrent glioblastoma: ROSALIE study. *JCO* 2022;40:2034.
67 Liu J, Fu M, Wang M, *et al*. Cancer vaccines as promising immuno-therapeutics: platforms and current progress. *J Hematol Oncol* 2022;15:28.
68 Sabado RL, Balan S, Bhardwaj N. Dendritic cell-based immunotherapy. *Cell Res* 2017;27:74–95.
69 Frey S, Castro A, Arsiwala A, *et al*. Bionanotechnology for vaccine design. *Curr Opin Biotechnol* 2018;52:80–8.
70 Percie du Sert N, Hurst V, Ahluwalia A, *et al*. The ARRIVE guidelines 2.0: Updated guidelines for reporting animal research. *PLoS Biol* 2020;18:e3000410.